RESEARCH ARTICLE

WILEY

Multilevel convergence of interoceptive impairments in hypertension: New evidence of disrupted body–brain interactions

Adrián Yoris[1,2] | Sofía Abrevaya[1,2] | Sol Esteves[1] | Paula Salamone[1,2] | Nicolás Lori[3,4,5] | Miguel Martorell[1] | Agustina Legaz[1] | Florencia Alifano[1] | Agustín Petroni[1,2,6,7] | Ramiro Sánchez[8] | Lucas Sedeño[1,2] | Adolfo M. García[1,2,9] | Agustín Ibáñez[1,2,10,11,12]

[1]Laboratory of Experimental Psychology and Neuroscience (LPEN), Institute of Cognitive and Translational Neuroscience (INCYT), INECO Foundation, Favaloro University, Buenos Aires, Argentina

[2]National Scientific and Technical Research Council (CONICET), Buenos Aires, Argentina

[3]Laboratory of Neuroimaging and Neuroscience (LANEN), INECO Neurosciences Oroño, Institute of Cognitive and Translational Neuroscience (INCYT), INECO Foundation, Favaloro University, Rosario, Argentina

[4]Diagnóstico Médico Oroño, Grupo Oroño, Rosario, Argentina

[5]ICVS/3Bs & Centre Algoritmi, University of Minho, Braga, Portugal

[6]Instituto de Ingeniería Biomédica, Facultad de Ingeniería, Universidad de Buenos Aires, Argentina

[7]Deptartamento de Computación, Universidad de Buenos Aires, Argentina

[8]Metabolic and Arterial Hypertension Unit, Favaloro Foundation Hospital, Buenos Aires, Argentina

[9]Faculty of Education, National University of Cuyo (UNCuyo), Mendoza, Argentina

[10]Universidad Autónoma del Caribe, Barranquilla, Colombia

[11]Center for Social and Cognitive Neuroscience (CSCN), School of Psychology, Universidad Adolfo Ibañez, Santiago, Chile

[12]Centre of Excellence in Cognition and its Disorders, Australian Research Council (ACR), Sydney, Australia

Correspondence
Agustín Ibáñez, Pacheco de Melo 1860, C1126AAB, Buenos Aires, Argentina.
Email: aibanez@ineco.org.ar

Funding information
CONICET; INECO Foundation; CONICYT/FONDECYT, Grant/Award Number: 1170010; FONCyT-PICT, Grant/Award Numbers: 2012-0412, 2012-1309; FONDAP, Grant/Award Number: 15150012

Abstract

Interoception, the sensing of visceral body signals, involves an interplay between neural and autonomic mechanisms. Clinical studies into this domain have focused on patients with neurological and psychiatric disorders, showing that damage to relevant brain mechanisms can variously alter interoceptive functions. However, the association between peripheral cardiac-system alterations and neurocognitive markers of interoception remains poorly understood. To bridge this gap, we examined multidimensional neural markers of interoception in patients with early stage of hypertensive disease (HTD) and healthy controls. Strategically, we recruited only HTD patients without cognitive impairment (as shown by neuropsychological tests), brain atrophy (as assessed with voxel-based morphometry), or white matter abnormalities (as evidenced by diffusion tensor imaging analysis). Interoceptive domains were assessed through (a) a behavioral heartbeat detection task; (b) measures of the heart-evoked potential (HEP), an electrophysiological cortical signature of attention to cardiac signals; and (c) neuroimaging recordings (MRI and fMRI) to evaluate anatomical and functional connectivity properties of key interoceptive regions (namely, the insula and the anterior cingulate cortex). Relative to controls, patients exhibited poorer interoceptive performance and reduced HEP modulations, alongside an abnormal association between interoceptive performance and both the volume and functional connectivity of the above regions. Such results suggest that peripheral cardiac-system impairments can be associated with abnormal behavioral and

neurocognitive signatures of interoception. More generally, our findings indicate that interoceptive processes entail bidirectional influences between the cardiovascular and the central nervous systems.

1 | INTRODUCTION

Interoception, the sensing of visceral body signals, involves an interplay between neural and autonomic mechanisms (Critchley & Harrison, 2013; Craig, 2002). In line with the brain-centered approach characterizing embodied cognition research (Barsalou, 2008; Birba et al., 2017; Craig, 2009; Gallese & Lakoff, 2005; Mahon & Caramazza, 2008; Seth, 2013), most clinical studies into this domain have focused on patients with neurological (Adolfi et al., 2016; Couto et al., 2015; García-Cordero et al., 2016; Khalsa, Rudrauf, Feinstein, & Tranel, 2009a; Yoris et al., in press) and psychiatric (Dunn, Dalgleish, Ogilvie, & Lawrence, 2007; Khalsa et al., 2015; Muller et al., 2015; Terhaar, Viola, Bär, & Debener, 2012; Yoris et al., 2015, 2017) disorders. This literature has revealed which interoceptive domains are distinctively affected following brain damage or dysfunction. Yet, several reports show that relevant interoceptive processes can also be disrupted in patients with heart conditions and autonomic disruptions (Gray et al., 2007; Gray, Rylander, Harrison, Wallin, & Critchley, 2009; Smith, Thayer, Khalsa, & Lane, 2017; Shivkumar et al., 2016), in line with current theoretical proposals such as the neurovisceral integration model (Smith et al., 2017).

However, the association among autonomic disruptions and interoception remains poorly understood, particularly because extant studies have failed to rule out accompanying neurocognitive alterations as key determinants of the observed deficits. Here, we bridge this gap by examining multidimensional neural markers of interoception in hypertensive disease (HTD) patients with well-preserved neurocognitive profiles. Insofar as interoceptive dynamics are not fully reducible to neural processes, this approach offers a novel opportunity to investigate peripheral aspects of such functions.

Indirect evidence suggests that significant interoceptive changes, even at a neural level, may be linked to cardiovascular alterations. For example, increases of heart rate and respiratory sensations induced by isoproterenol infusions are associated with greater interoceptive perception (Khalsa et al., 2009a) and even with activation of the insula, a key hub of this domain (Hassanpour et al., 2016; Oppenheimer & Cechetto, 2016; Schulz, 2016). Moreover, interoceptive changes are associated with modulations of cardiovascular states due to isometric exercise (Pollatos, Herbert, Kaufmann, Auer, & Schandry, 2007b), stress (Fairclough & Goodwin, 2007), and blood pressure increases (Fahrenberg, Franck, Baas, & Jost, 1995). Further support is provided by an exceptional case of a patient with an extracorporeal left-univentricular cardiac assist device (a man with "two hearts"). During a heartbeat detection (HBD) task, the patient was capable of tracking the beats of an external pump but not those of his own heart, with reduced modulations of a relevant cortical marker called heart-evoked potential (HEP) (Couto et al., 2013). Also, previous research has revealed differences between untreated HTD patients and normotensive subjects during heartbeat discrimination (Koroboki et al., 2010) and blood pressure estimation (Fahrenberg et al., 1995) tasks. Importantly, these studies did not consider the patients' neuropsychological or neurological status, thus proving blind to the possible impact of neurocognitive impairment on the results.

Although HTD has been associated with cognitive decline (Kilander, Nyman, Boberg, Hansson, & Lithell, 1998; Launer, Masaki, Petrovitch, Foley, & Havlik, 1995; Starr, Whalley, Inch, & Shering, 1993; Tzourio, Dufouil, Ducimetiere, & Alperovitch, 1999) and white matter lesions (De Leeuw et al., 2001; de Leeuw et al., 2002), these alterations manifest quite variedly. In fact, several works have reported HTD samples with normal cognitive performance (Farmer et al., 1990; Scherr, Hebert, Smith, & Evans, 1991; Van Boxtel et al., 1997) and white matter preservation as measured via diffusion tensor imaging (DTI) (Farmer et al., 1990; Gons et al., 2010; Hannesdottir et al., 2009; Nitkunan, Charlton, Mcintyre, Barrick, Howe, & Markus, 2008; Scherr et al., 1991; Van Boxtel et al., 1997). Such a scenario allowed us to select a neurocognitively preserved HTD sample which, though not representative of the entire HTD population, offered a suitable model of cardiovascular disturbances without major central nervous system impairments.

Taken together, this evidence indirectly suggests that neurocognitive markers of interoception could be associated with cardiovascular deficits. Here, we offer the first direct testing of this hypothesis by examining behavioral, neurophysiological, gray matter volume, and functional connectivity signatures of interoception in healthy subjects and HTD patients without neurocognitive alterations (featuring no cognitive deficits, gray matter abnormalities, or white matter alterations). In particular, our multidimensional approach comprised analyses of (a) behavioral performance on a validated HBD task (Canales-Johnson et al., 2015; Couto et al., 2013; Yoris et al., 2015, 2017); (b) ongoing modulations of the HEP, an electrophysiological cortical signature modulated by attention to cardiac signals (García-Cordero et al., 2016; Yoris et al., 2017; Terhaar et al., 2012); and (c) neuroimaging recordings, to evaluate anatomical and functional connectivity properties of key interoceptive regions, namely: the insula, the anterior cingulate cortex (ACC), and the somatosensory cortex (Adolfi et al., 2016; Craig, 2002; Critchley, Wiens, Rotshtein, Ohman, & Dolan, 2004; Fukushima, Terasawa, & Umeda, 2011; Hassanpour et al., 2016). In light of the above considerations, we predicted that HTD patients would exhibit

TABLE 1 Demographic, cardiovascular, neuropsychological, and mood measures

Variables	Groups HTD patients	Controls	Statistics
a. Demographic results			
Gender (F:M)	12:12	17:9	$\chi2 = 0.89$, $p = .34$
Age	67.86 (9.09)	65.92 (7.51)	$F = 0.64$, $p = .42$, $\eta p^2 = 0.01$
Education	15.59 (4.09)	16.72 (2.18)	$F = 0.68$, $p = .30$, $\eta p^2 = 0.01$
Body mass index	26.36 (33.16)	25.39 (3.27)	$F = 1.07$, $p = .30$, $\eta p^2 = 0.02$
Handedness (R:L)	24:0	25:1	—
b. Cardiovascular assessment Clinical measures			
ABPM (systolic 24 h)	131.33 (10.72)	112.72 (15.67)	$F = 5.57$, $p = .02^*$, $\eta p^2 = 0.14$
OBP systolic	148.47 (18.80)	134.04 (14.99)	$F = 9.83$, $p < .01^*$, $\eta p^2 = 0.16$
OBP diastolic	81.82 (8.91)	75.78 (9.01)	$F = 1.81$, $p = .03^*$, $\eta p^2 = 0.09$
Cardiac measures in HBD task			
HR	76.93 (25.52)	69.06 (9.94)	$F = 1.15$, $p = .28$, $\eta p2 = 0 .03$
HRV HF	57.79 (22.43)	55.63 (2.10)	$F = 0.13$, $p = .70$, $\eta p2 = 0.00$
HR LF	42.99 (22.71)	44.34 (17.55)	$F = 0.75$, $p = .38$, $\eta p2 = 0.01$
HRV HF/LF	3.07 (3.90)	2.21 (2.10)	$F = 0.92$, $p = .34$, $\eta p2 = 0.02$
c. Neuropsychological assessment			
IFS global score	23.92 (3.83)	25.04 (2.41)	$F = 1.39$, $p = .24$, $\eta p2 = 0.03$
IFS (working memory sub-index)	7.28 (2.00)	7.04 (2.05)	$F = 0.16$, $p = .68$, $\eta p2 = 0.00$
IFS (motor programing sub-index)	2.90 (0.29)	2.91 (0.28)	$F = 0.00$, $p = .92$, $\eta p2 = 0.00$
RAVL (global Score)	37.8 (8.53)	41.86 (11.72)	$F = 1.07$, $p = .30$, $\eta p2 = 0.02$
d. Mood and anxiety results			
BDI-II	9.5 (4.85)	11.78 (9.50)	$F = 0 .59$, $p = .44$, $\eta p^2 = 0.02$
STAI-T	34.83 (7.20)	30.00 (3.62)	$F = 5.4$, $p = .02^*$, $\eta p^2 = 0 .16$
STAI-S	28.73 (6.08)	26.64 (3.62)	$F = 1.13$, $p = 29$, $\eta p2 = 0.03$

Note. Abbreviations: ABPM: ambulatory blood pressure monitor; OBP: office blood pressure; HR: heart rate; HRV HF: heart rate variability (high frequency); HRV LF: heart rate variability (low frequency); IFS: INECO Frontal Screening battery; BDI-II: Beck Depression Inventory; STAI-S/T: State/Trait Anxiety Index.
Results are presented as mean (*SD*). The asterisk indicates significant differences.

behavioral interoceptive deficits and alterations in key neural correlates of such a domain.

2 | METHODS

2.1 | Participants

The study comprised 50 participants, namely, 24 (12 female) patients with essential HTD and 26 (17 female) healthy controls. Subjects in the HTD group were chronic outpatients of the Metabolic and Arterial Hypertension Unit of the Favaloro Foundation Hospital, and they were diagnosed following current revised criteria (Sanchez et al., 2003). Their blood pressure fell in Grade 1, within the hypertension range (Mancia

et al., 2007). The patients' condition was confirmed by office blood pressure (OBP) readings and ambulatory blood pressure monitoring (ABPM) (for details, see Table 1). None of the patients presented cognitive impairments (see section "Neuropsychological measures" in Table 1), lacunar infarcts, white or grey matter lesions (Supporting Information, Figures 1 and 2), or psychiatric diseases. Psychiatric features were assessed following WHO's ICD-10 diagnostic guidelines (WHO, 1992). All patients presenting relevant symptoms were excluded from the study. Also, while all the patients in the final sample were under antihypertensive medication, intake was suspended 48 hs. before the study to prevent drug-related confounds (Supporting Information, Table 1). The control sample was matched for age, gender, education, handedness, and body mass index with the HTD group (Table 1). These

subjects presented no history of drug abuse, neuropsychiatric disease, cognitive impairment or hypertension. All participants provided informed consent in accordance with the Declaration of Helsinki. The study was approved by the institutional ethics committee.

3 | CLINICAL AND BEHAVIORAL ASSESSMENT

3.1 | Neuropsychological measures

Executive functions were assessed with the INECO Frontal Screening (IFS) battery (Torralva, Roca, Gleichgerrcht, Lopez, & Manes, 2009), which taps eight relevant domains, including motor programming, inhibitory control, and working memory. Additionally, the Rey Auditory Verbal Learning test (RAVL) (Schmidt, 1996) was used as measure of short-term verbal memory.

3.2 | Mood and anxiety measurements

Considering the relation between emotional states and interoception (Ko et al., 2002; Raglin & Morgan, 1987; Räikkönen, Matthews, Flory, Owens, & Gump, 1999; Sullivan et al., 1981), we also examined anxiety and mood symptoms. Anxiety was evaluated by the State-Trait Anxiety Inventory (STAI) (Spielberger & Vagg, 1984), which involves one trait anxiety index and one state anxiety scale. Depression symptoms were assessed with Beck's Depression Inventory (BDI-II) (Beck, Steer, Ball, & Ranieri, 1996), a dimensional measure of the participants' affective state the week before the assessment.

3.3 | Interoceptive performance: Heartbeat detection task

Cardiac interoception was assessed through a modified version of a validated HBD task (Couto et al., 2013; García-Cordero et al., 2016; Melloni et al., 2013; Sedeno et al., 2014; Yoris et al., 2015, 2017), encompassing two conditions. In the exteroceptive condition (EC), a control measure of external monitoring skills, participants tapped a keyboard to follow binaurally presented heartbeats. This condition included two blocks of 2.5 min, featuring regularly timed and irregularly timed heartbeats, respectively. In the interoceptive condition (IC), aimed to assess inner signal monitoring, participants tapped a key to follow their own heartbeats without any external cues. Each participant completed two 2.5-min blocks. The IC provides a measure of interoceptive accuracy, namely, the subjects' objective performance in following their own heartbeats (Garfinkel, Seth, Barrett, Suzuki, & Critchley, 2015). During all blocks, participants were requested to respond with their dominant hand, to keep their eyes on a fixation cross, and to avoid excessive blinking and moving while the latter remained on screen.

Behavioral performance was analyzed for each subject through a modified version of Schandry's (Schandry, 1981) precision index (Couto et al., 2015; García-Cordero et al., 2016; Melloni et al., 2013; Yoris et al., 2015, 2017). This index is based on two scores, namely, correct answers and recorded heartbeats. The former refers to the total

number responses that matched each of the subject's heartbeats. To estimate this match, every motor response is compared within a time window around every recorded heartbeat; if the tap input is temporally locked within any heartbeat, that response is considered as correct—the procedure to estimate the time window for each subject is detailed in Melloni et al. (2013). On the other hand, recorded heartbeats refer to the total number of heartbeats recorded in each condition. Both scores were used to calculate behavioral accuracy, following this equation:

$$1 - \frac{(\text{Recorded heartbeats} - \sum \text{Correct answers})}{\text{Recorded heartbeats}}$$

This precision index can vary between 0 and 1, with higher scores indicating only small differences between correct answers and recorded heartbeats, and, thus, better performance.

In addition, to ensure that our results were not biased by the discrimination between correct and wrong answers, we also estimated the subjects' accuracy based on their total number of responses. We calculated an index similar to the one used by (Schandry, 1981), in which total numbers of responses (mental counting, in the case of Schandry, tapping in our study) were adjusted by the total number of heartbeats, and then compared between groups.

3.4 | Heart rate, heart rate variability, and blood pressure during the HBD task

We performed complementary analyses to assess the influence of cardiodynamic differences between samples during the HBD task. This is important to assess an impact of moment-to-moment differences on our results, so that they can be reliably associated to chronic alterations of the peripheral system. To this end, we compared the two samples' heart rate (HR), heart rate variability (HRV), and systolic/diastolic blood pressure (BP) during the task. Regarding HR and HRV, we imported the beat-to-beat RR interval data from the ECG (using the Matlab platform) to the Kubios HRV program (Tarvainen, Niskanen, Lipponen, Ranta-Aho, & Karjalainen, 2013). This software automatically analyzes HRV in both time and frequency domains, generating a spectral power analysis for different frequency bands: high frequency (HF) and low frequency (LF). The HF component occurs at the frequency of adult respiration (from 15 to 40 Hz) and primarily reflects cardiac parasympathetic influence due to respiratory sinus arrhythmia. The LF component occurs within 0.04 and 0.15 Hz. The LF/HF ratio has been suggested to mirror sympatho/vagal balance (Eckberg, 1997). The Kubios HRV also gives a mean HR measure for each condition. Finally, BP was measured immediately after the HBD task using an office monitor. One index was obtained with the format systolic/diastolic measure.

3.5 | Clinical and behavioral data analysis

Demographic, neuropsychological, and clinical data were assessed through ANOVAs. Gender was analyzed with the Pearson chi-squared (χ^2) test. Performance on the HBD task was scrutinized via repeated measures ANOVA (with the two conditions as a within-subject factor and groups as a between one). Also, considering the possible influence of anxiety symptoms on interoception (Pollatos, Gramann, & Schandry,
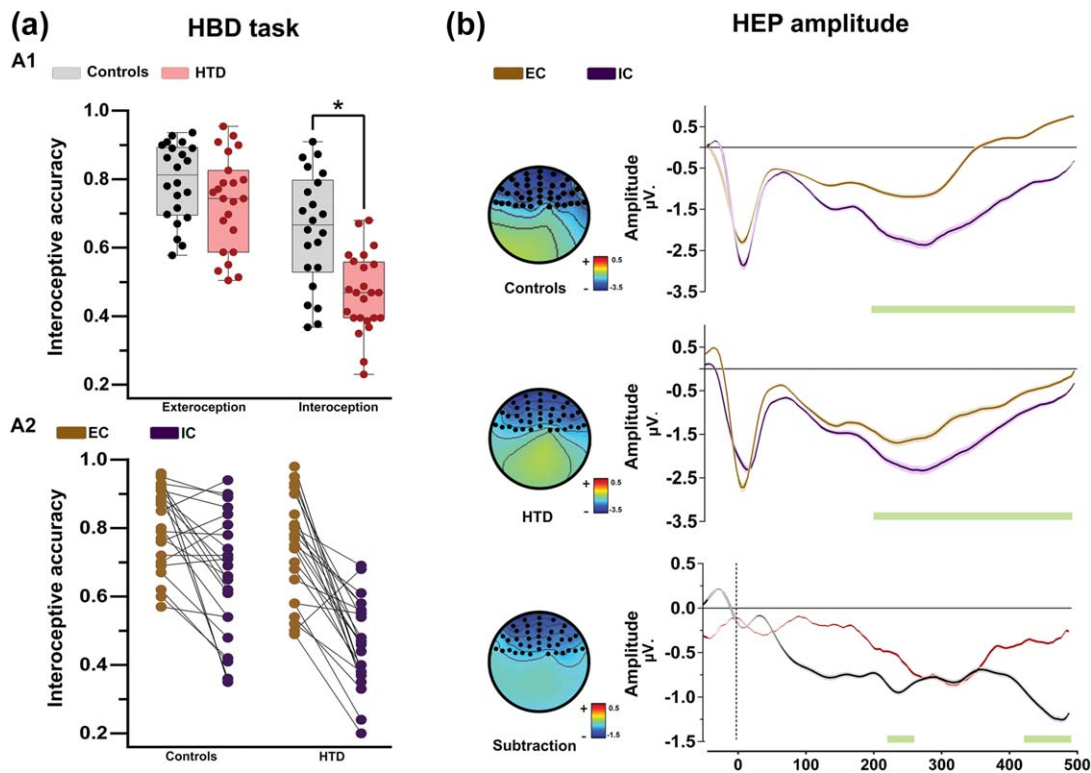
FIGURE 1 Behavioral performance and HEP modulations in the HBD task. (a) Behavioral performance of patients and controls. (A1) The asterisk indicates significant differences ($p < .05$). Individual performance is represented inside and outside of the box as dark points. The middle box line indicates the group's mean values. The precision score can vary between 0 and 1, with higher scores indicating better performance. (A2) Individual performance comparison between conditions (per group). (b) HEP analysis. All differences reported were calculated via Monte Carlo permutations analysis (5000 permutations, $p < .05$) point by point (Manly, 2007). A minimum extension of five consecutive points was selected as criteria to graph clusters. Shadowed lines indicate SEM. Green bars indicate significant differences. HTD: hypertensive disease; EC: exteroceptive condition; IC: interoceptive condition [Color figure can be viewed at wileyonlinelibrary.com]

2007a; Pollatos & Schandry, 2004) and the significant mood differences between groups (Table 1), we performed an ANCOVA using STAI (trait subscale) scores as covariates for the HBD measures. Effect sizes were reported with partial eta squared (η_p^2). Also, to confirm the robustness of our negative results in HR, HRV, and blood pressure during the HBD task, we established the probability with which the null hypothesis can be accepted or rejected via a Bayes analysis on JASP Statistical Software (https://jasp-stats.org/, JASP Team (2017) (Version 0.8.2); (Rouder, Speckman, Sun, Morey, & Iverson, 2009). We performed Bayes tests for all results yielding non-significant differences (Dienes, 2011, 2014; Dienes, Coulton, & Heather, 2017; Dienes & Mclatchie, 2017). A Bayes factor of 0 to 0.33 strongly supports the null hypothesis, whereas a Bayes factor between 0.33 and 3 indicates insufficient evidence to do so. Finally, Bayes scores above 3 support the alternative hypothesis.

4 | ERP MEASURES

4.1 | EEG signal acquisition and preprocessing

During the HBD task, we recorded HD-EEG signals with a Biosemi Active-two 128-channel system at 1024 Hz, resampled offline at 256 Hz. Two external electrodes were included to record ECG data. The data were band-pass filtered during recording (0.1–100 Hz) and offline (0.3–50 Hz) to remove undesired frequency components. The reference was set by default to link mastoids, and rereferenced offline to the average electrodes. EEG data were segmented between −200 and 500 ms. Segments with eye movement contamination were removed from further analysis using independent component analysis (ICA) and a visual inspection procedure. The epochs were baseline-corrected (baseline: −200 ms to 0 ms) (Szczepanski et al., 2014). Noisy epochs were rejected from the analysis using a visual inspection procedure as in previous studies (García-Cordero et al., 2016).

4.2 | Heart-evoked potential

The HEP is a modulation emerging 200–500 ms after the R-wave peak (Canales-Johnson et al., 2015; Fukushima et al., 2011; Montoya, Schandry, & Muller, 1993; Pollatos & Schandry, 2004; Yoris et al., 2017). It is considered an automatic cortical signature of interoceptive signals (Pollatos, Kirsch, & Schandry, 2005a; Schandry & Montoya, 1996) that is modulated by attention to heartbeats (Fukushima et al., 2011; García-Cordero et al., 2016; Terhaar et al., 2012; Yoris et al., 2017). The HEP was obtained by sampling EEG epochs time-locked to the R-wave. To avoid the influence of cardiac field artifacts (CFAs) (Kern, Aertsen, Schulze-Bonhage, & Ball, 2013), we analyzed the HEP signal with a
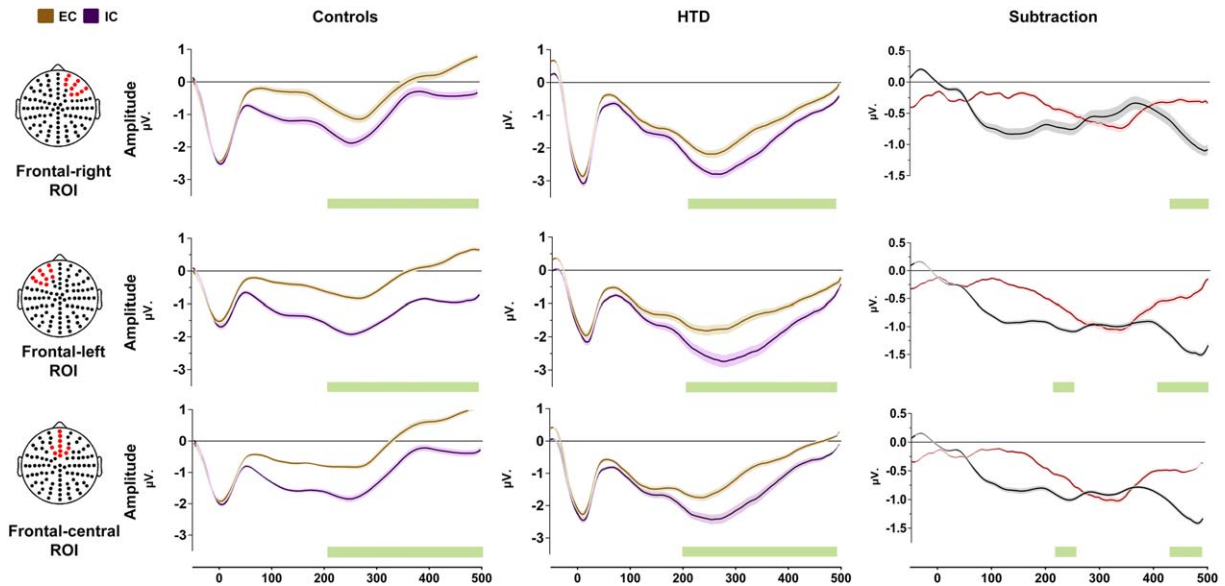
FIGURE 2 HEP amplitude in three regions of interest (ROIs): central frontal ROI, left frontal ROI, and right frontal ROI. All differences reported were calculated via Monte Carlo permutations analysis (5000 permutations, $p < .05$) by point (Manly, 2007). Shadowed lines indicate SEM. Green bars indicate significant differences. Yellow dots in the channel location diagrams illustrate the electrodes included in each ROI [Color figure can be viewed at wileyonlinelibrary.com]

point-by-point permutation analysis only after the 200-ms mark (see below), as previous reports suggested a possible contamination of the signal by the CFA before this time (Kern et al., 2013; Park, Correia, Ducorps, & Tallon-Baudry, 2014).

4.3 | ERP data analysis

In light of the frontal topography of the HEP (Fukushima et al., 2011; Gray et al., 2007; Pollatos & Schandry, 2004), and following previous reports of our group (Couto et al., 2015; García-Cordero et al., 2016; Yoris et al., 2017), HEP analysis was performed considering a frontal region of interest (ROI) (41 frontal electrodes, see Figure 1). Based on previous reports (García-Cordero et al., 2016; Pollatos, Kirsch, & Schandry, 2005b; Pollatos & Schandry, 2004), we selected three additional ROIs for analysis: a right frontal ROI (Biosemi C3, C4, C5, C6, C7, C9, C10, C13, C14, C15); a left frontal ROI (Biosemi C26, C27, C28, C31, C32, D3, D4, D5, D6, D7); and a centro-frontal ROI (Biosemi C11, C12, C18, C19, C20, C21, C22, C23, C24, C25) (Figure 2). Moreover, given the relation between interoception and the somatonsesory cortex (Craig, 2002; Critchley et al., 2004; Couto et al., 2013; Khalsa et al., 2009a), and based on previous studies (Fukushima et al., 2011; Leopold & Schandry, 2001; Pollatos et al., 2005b), we tested more latero-posterior ROIs (each one in the left and right hemisphere), namely, a left fronto-lateral ROI (Biosemi D11, D12, D13, D14, D17, D18, D19, D20, D27, D28) and a right fronto-lateral ROI (Biosemi B17, B18, B19, B20, B21, B22, B23, B30, B1, B2) (Supporting Information, Figure 4).

Point-by-point comparisons along the ERP signal were made via the Monte Carlo permutation test (5000 permutations, $p < .05$) (Manly, 2007), as done in previous HEP studies (Couto et al., 2015; García-Cordero et al., 2016; Yoris et al., 2017) and other ERP studies (Amoruso et al., 2014; Andrillon, Kouider, Agus, & Pressnitzer, 2015;

Naccache et al., 2005). This method circumvents the multiple comparisons problem and does not depend on multiple comparison corrections or Gaussian distribution assumptions (Nichols & Holmes, 2002). In addition, it avoids the selection of narrow a-priori windows for analysis, preventing circularity biases. Finally, and following recommendations for t test analyses (Lakens, 2013), we calculated effect sizes with Cohen's d. This statistic is recommended for measuring the magnitude of differences for independent sample t tests (Cohen, 1988), namely, the statistical method used in each permutation step. By comparing HEP modulations in the IC vs the EC of the HBD task, we obtained the t-value of each point in the significant windows of the HEP, both for controls and HTD. Similarly, a recommended formula was calculated to compare independent samples (i.e., contrasting the HEP subtraction in both groups). Depending on the value of d, effect sizes can be considered small (0–0.20), medium (0.50–0.80), or large (>0.80) (Cohen, 1988). First, we calculated the effect size of the differences between conditions at each time-point and then we averaged the effect sizes in the significant window.

5 | MRI MEASURES

5.1 | Image acquisition

MRI acquisition and preprocessing steps are reported following the practical guide from the Organization for Human Brain Mapping (OHBM) (Nichols et al., 2017; Poldrack et al., 2017). Subjects were scanned in a 1.5 T Phillips Intera scanner with a standard head coil (8 channels). We acquired whole-brain T1-weighted anatomical 3D spin echo volumes, parallel to the plane connecting the anterior and posterior commissures, with the following parameters: repetition time (TR) = 7489 ms; echo time (TE) = 3420 ms; flip angle = 8°; 196 slices,

matrix dimension = 256 × 240; voxel size = 1 × 1 × 1 mm³; sequence duration = 7 min. Also, T2 and FLAIR sequences were acquired to improve the detection of lesion or atrophy in each group. In addition, we obtained whole-brain diffusion images with a twice-refocused, single-shot, echo-planar imaging pulse sequence, in the same plane as the T1-weighted images. We used the following parameters: TR = 11,468 ms; TE = 75 ms; flip angle = 90°; 65 slices, matrix dimension = 112 × 112; voxel size = 2 × 2 × 2 mm³; sequence duration = 20 min. The tensor was computed using 32 noncollinear diffusion directions (b = 800 s/mm²) that were maximally spread by considering the minimal energy arrangement of point charges on a sphere, and one scan without diffusion weighting (b = 0 s/mm², b0). Finally, functional spin echo volumes, parallel to the anterior–posterior commissures, covering the whole brain, were sequentially and ascendingly acquired with the following parameters: TR = 2777 ms; TE = 50 ms; flip angle = 90°; 33 slices, matrix dimension = 64 × 64; voxel size in plane = 3.6 mm × 3.6 mm; slice thickness = 4 mm; sequence duration = 10 min; number of volumes = 209. For acquisition, participants were asked not to think about anything in particular, to keep their eyes closed, and to avoid moving or falling asleep. We chose the closed-eyes modality to avoid noisy signals coming from the visual cortex (Zou et al., 2015) and to facilitate attention to interoceptive sensations (Xu et al., 2014; Wang, Li, Xu, & Ding, 2015).

The final sample for MRI analyses consisted of 21 controls and 20 patients. The rest of the participants were discarded due to the following reasons: (a) absence of imaging data (e.g., some participants refused to undergo the scanning process adducing claustrophobia), (b) artifacts or acquisition mistakes established through visual inspection of the data, and/or (c) excessive head motion (movements greater than 3 mm and/or rotations higher than 3°). Groups were still matched in terms of age, gender, education, and body mass index (Supporting Information, Table 2).

5.2 | Neurocognitive status analysis

To confirm that HTD patients did not present any brain structural alterations, we assessed gray and white matter integrity via voxel-based morphometry (VBM) and DTI, relative to controls. We also evaluated whether samples presented whole-brain functional connectivity differences based on an interoceptive seed (selected from the results of the association between VBM and interoceptive accuracy; see section "Association between interoceptive and neuroimaging measures"). For VBM analysis, data were preprocessed on the DARTEL Toolbox following validated procedures (Ashburner & Friston, 2000; García-Cordero et al., 2016; Melloni et al., 2016; Sedeno et al., 2017) via Statistical Parametric Mapping software (SPM12) (http://www.fil.ion.ucl.ac.uk/spm/software/spm12/). T1-weighted images in native space were first segmented using the default parameters of the SPM12 (bias regularization was set to 0.001 and bias FWHM was set to 60 mm cutoff) into white matter (WM), grey matter (GM), and cerebrospinal fluid (CFS) (these three tissues were used to estimate the total intracranial volume, TIV). Then, we ran the "DARTEL (create template)" module using the GM and WM segmented images—with the default parameters indicated by the SPM12—

to create a template that is generated from the complete data set (increasing the accuracy of inter-subject alignment) (Ashburner, 2007). Next, we used the "Normalise to MNI Space" module from DARTEL Tools to affine register the last template from the previous step into the MNI Space. This transformation was then applied to all the individual GM segmented scans to also be brought into standard space. Subsequently, all images were modulated to correct volume changes by Jacobian determinants, and to avoid bias in the intensity of an area due to its expansion during warping. Finally, an isotropic Gaussian kernel of 12-mm full-width at half-maximum was applied to all images. The size of the kernel was selected based on previous recommendations (Ashburner & Friston, 2000; Good et al., 2001), suggesting that it favors more normal data distributions for subsequent parametric analysis. We accounted for the global atrophy pattern via a t test between groups, corrected by TIV (SPM12). Statistical significance was set at $p < .001$ uncorrected, extent threshold = 50 voxels (Abrevaya et al., 2017; Garcia et al., 2017; García-Cordero et al., 2016; Irish, Piguet, Hodges, & Hornberger, 2014; Melloni et al., 2015; Santamaria-Garcia et al., 2017; Sedeno et al., 2014, 2016). Finally, to establish the robustness of VBM differences between groups, we calculated their Cohen's d based on the total grey volume per area estimated via the AAL atlas (Tzourio-Mazoyer et al., 2002).

For DTI analysis, data were processed on the FMRIB Software Library (FSL 5.0.7) (Smith et al., 2004). First, to correct motion artifacts and eddy-current distortions, each DTI volume was affine-aligned to its corresponding b0 image via a FSL's linear registration tool (FLIRT v6) (Jenkinson & Smith, 2001). Then, using the brain extraction tool (BET2, with fractional threshold = 0.1 and vertical gradient = 0) (Smith, 2002), we generated a brain mask of each b0 image. Next, for fitting the tensor and computing the diagonal elements (λ_1, λ_2, λ_3) at each voxel, we employed the FSL's diffusion toolbox (FDT v2.0) (Behrens et al., 2003). From this estimation, fractional anisotropy (FA) and mean diffusivity (MD) were generated. Voxel-wise statistical analysis of the FA and MD data was performed using the Tract-Based Spatial Statistics (TBSS v1.2) (Smith et al., 2006). Each data was affine-aligned into MNI 152 standard space using the nonlinear registration tool FNIRT (Anderson, Jenkinson, & Smith, 2007). Then, all the normalized FA images (from patients and controls) were averaged to create a mean FA template, which was thinned to generate a FA skeleton representing the centers of all tracts common to both groups. All subjects' aligned FA and MD images were then projected onto this skeleton and, to compare them between groups, we performed a voxel-wise permutation test via FSL's randomize tool (Winkler, Ridgway, Webster, Smith, & Nichols, 2014) with 5000 permutations, considering a statistical threshold of $p < .001$ uncorrected, extent threshold = 50 voxels. As for the VBM analysis, we estimated the effect size via Cohen's d, based on the calculation of the mean FA and MD from the regions of interest of the JHU DTI-based white-matter atlases (https://fsl.fmrib.ox.ac.uk/fsl/fslwiki/Atlases).

For functional connectivity differences, resting-state fMRI scans were preprocessed using the Data Processing Assistant for Resting-State fMRI (DPARSF V2.3) (Chao-Gan & Yu-Feng, 2010), an open-access toolbox that generates automatic analysis pipelines for imaging data. For each preprocessing step, DPARFS called the Statistical Parametric Mapping (SPM 12) and the Resting-State fMRI Data Analysis
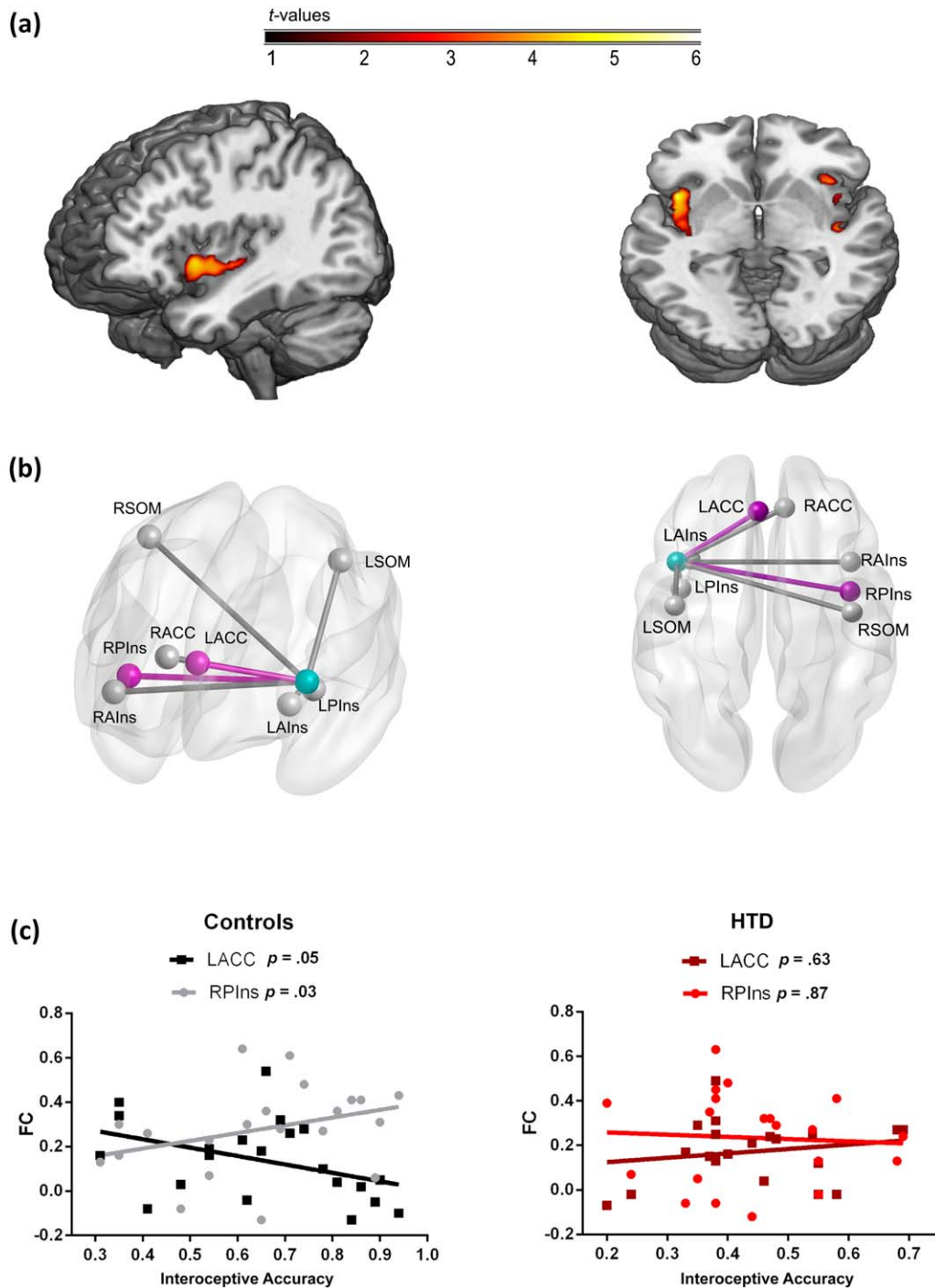
FIGURE 3 Association between interoceptive and MRI measures. (a) Linear regression between gray matter volume and performance during the IC in favor of the control group. Brain images are presented according to neurological convention. (b) Seed analysis associated to interoceptive performance in controls. The light blue node represents the left insular seed. Pink nodes and edges represent the connections with the seed that were significantly associated with IC (Spearman's correlations) in controls. L: left; R: right; P: posterior; A: anterior; Ins: insula; ACC: anterior cingulated cortex; SOM: somatosensory cortex. (c) Scatter plots of the significant associations from panel B for both controls and HTD patients

Toolkit (based on default functions of the REST V.1.7 toolbox). Before preprocessing, the first five volumes of each subject's resting-state session were discarded to ensure that magnetization achieved a steady state. Then, images were slice-time corrected (using as reference the middle slice of each volume) and aligned to the first scan of the session

to correct for head movement (SPM functions). To reduce the effect of motion and physiological artifacts (such as cardiac and respiration effects), six motion parameters, CFS, and WM signals were removed as nuisance variables (REST V1.7 toolbox). CFS and WM masks for this procedure were derived from the tissue segmentation of each subject's

TABLE 2   Regression between grey matter in interoceptive regions and interoceptive accuracy in controls

Brain region	Cluster k	Peak t	Peak z	Peak p (uncl)	x	y	z
Left insula	562	5.84	4.37	<.001	−42	12	−4.5[a]
		3.91	3.31	<.001	−36	−18	0
Superior temporal gyrus		3.90	3.30	<.001	−42	−9	−6
Right insula	162	5.08	3.99	<.001	28.5	12	−18
		4.01	3.37	<.001	30	24	−21
Right insula	152	4.39	3.60	<.001	34.5	19.5	−7.5
		3.97	3.35	<.001	40.5	18	−1.5
		3.61	3.11	<.001	27	24	−7.5
Right insula	107	4.15	3.46	<.001	39	−16.5	0
Right insula	60	3.88	3.29	<.001	37.5	0	3

[a]This peak was selected to create the seed for the functional connectivity analysis. Reported areas are based on the Automated Anatomical Labeling atlas (Tzourio-Mazoyer et al., 2002).

T1 scan in native space with SPM12 (after co-registration of each subject's structural image with the functional image). Next, functional images were normalized to the MNI space using the echo-planar imaging (EPI) template from SPM (Ashburner & Friston, 1999), and then they were smoothed using an 8 mm full-width-at-half-maximum isotropic Gaussian kernel (SPM functions). Finally, data was band-pass filtered between 0.01-0.08 Hz given the relevance of slow frequency in the analysis of resting-state networks (Fox et al., 2005; Raichle, 2009) (REST V.1.7 toolbox).

Participants showed movements no greater than 1.5mm and/or rotations higher than 1.5° (Supporting Information, Table 2). As seed for the analysis, we selected the peak that presented the largest association between IC performance and gray matter volume in the control sample (see below, section "Association between interoceptive and neuroimaging measures", and also Figure 3 and Table 2). This seed was located in short gyri of the left insula ($x = -42$, $y = 12$, $z = -5$). The aim of this analysis was to evaluate whether groups presented differences in whole-brain functional connectivity relative to this interoceptive hub. For each participant, we extracted the BOLD signal time-course from the voxels within the seed region. To obtain a functional connectivity map, we then correlated these data to every voxel in the brain using Pearson's correlation coefficient via the DPARSF toolbox. Afterward, we performed a Fisher z-transformation. Then, the voxel-wise connectivity of these maps was compared between controls and HTD patients with a two-sample t test ($p < .001$ uncorrected, extent threshold = 50 voxels), on SPM12. In addition, Cohen's d was calculated based on the mean connectivity of each region of the AAL Atlas (Tzourio-Mazoyer et al., 2002).

In addition, we performed Bayes tests for all results yielding nonsignificant differences (Dienes, 2011, 2014; Dienes et al., 2017; Dienes & Mclatchie, 2017), to establish the probability with which the null hypothesis can be accepted or rejected. This calculation was performed for the structural (DTI, VBM) and functional connectivity differences between groups. To perform the VBM and functional connectivity comparisons between groups, we calculated total grey matter volume and the mean functional connectivity per area following the AAL atlas (Tzourio-Mazoyer et al., 2002), respectively. In the case of DTI, we used the mean FA and MD values from the JHU DTI-based white-matter atlases (https://fsl.fmrib.ox.ac.uk/fsl/fslwiki/Atlases).

5.3 | Association between interoceptive and neuroimaging measures

We evaluated whether controls and HTD patients presented different patterns of association between accuracy in the IC and both structural (VBM) and functional connectivity (seed analysis) properties of key interoceptive areas, namely, the bilateral anterior and posterior insula, the ACC and the somatosensory cortex (Adolfi et al., 2016; Craig, 2002; Critchley et al., 2004; Hassanpour et al., 2016).

5.3.1 | VBM analyses

To determine the correlation between morphometry and behavior, we performed a linear regression analysis with the IC accuracy score for each group on SPM 12. For this analysis, we restricted the analysis to the key interoceptive areas (bilateral anterior and posterior insula, ACC, and somatosensory cortex) by applying a binary mask. As reported in previous works (Garcia et al., 2017; García-Cordero et al., 2016; Irish et al., 2014), we applied a spatial threshold of 50 voxels, and an uncorrected statistical threshold of p values smaller than .001.

5.3.2 | Seed analyses

To test for the association between behavioral performance and correlation maps of the interoceptive network from the left insula seed (see "Neurocognitive status analysis" for the full description of preprocessing procedures), we first averaged the correlation values within the main hubs of this network for each participant, as done in previous studies (e.g., Abrevaya et al., 2017; Hoekzema et al., 2014; Mayer, Mannell, Ling, Gasparovic, & Yeo, 2011; Wu et al., 2011a,b). To this end, we selected four pre-defined bilateral regions from the AAL atlas

(Tzourio-Mazoyer et al., 2002): the anterior and posterior insula (Sedeno et al., 2016), the ACC, and the somatosensory cortex (henceforth designated as ROIs). Finally, we performed a Spearman correlation analysis between these connectivity values and the IC accuracy scores for each sample (the alpha level was set at $p < .05$, uncorrected). In addition, Cohen's d was calculated based on the mean connectivity of each region of the AAL Atlas (Tzourio-Mazoyer et al., 2002).

6 | RESULTS

6.1 | General neurocognitive status

No statistically significant differences between groups were observed on the IFS (including motor programing and working memory subindexes) or on the RAVL (verbal memory) test (Table 1). Neither did the groups differ in their state anxiety scores, although patients showed higher scores in the trait anxiety subscale (Table 1).

Finally, no significant between-group differences emerged in the VBM analysis (p-value $< .001$ uncorrected, spatial threshold = 50 voxels; see Supporting Information, Figure 1), in FA or MD from our DTI analyses ($p < .001$ uncorrected, spatial threshold = 50 voxels; see Supporting Information, Figure 2), or in the functional connectivity comparison based on the voxel-wise correlation of the short gyri of the left insula and the rest of the brain (p value $< .001$ uncorrected, spatial threshold = 50 voxels; see Supporting Information, Figure 3). In all these neuroimaging analyses, the Bayes factor was under 1 and, in most cases, between 0 and 0.33, supporting the null hypothesis (Dienes, 2014; Dienes & Mclatchie, 2017), namely, that there were no significant differences between groups (Supporting Information, Tables 3 and 4). In sum, convergent behavioral, VBM, DTI, and functional connectivity results revealed preserved cognitive and brain profiles in the patients.

6.2 | Behavioral results

6.2.1 | HBD task

We found a main effect of condition [$F = 28.8$, $p < .01$, $\eta p^2 = .41$], indicating higher performance in the EC than the IC. Finally, results showed an interaction between group and condition [$F = 4.18$, $p = .04$, $\eta p^2 = .08$] (Figure 1a). Post-hoc comparisons via Tukey's HSD [$MS = .02$, $df = 89.63$] showed that both groups performed similarly in the EC ($p = .54$, $\eta p^2 = .02$), whereas HTD patients were outperformed by controls in the IC ($p < .01$, $\eta p^2 = .24$). The latter difference remained significant after covariation with STAI-T scores ($F = 10.11$, $p < .01$, $\eta p^2 = .27$). Finally, using Schandry's index (Schandry, 1981), we also analyzed the subjects' performance considering their total number of responses, without discriminating between right and wrong ones. We found a group effect in the IC ($F = 5.92$, $p = .01$, $np^2 = 0.11$), such that controls ($M = 102.9$, $SD = 31.25$) outperformed HTD patients ($M = 85.04$, $SD = 28.57$). No group differences were found in the EC ($F = 0.12$, $p = .31$, $np^2 = 0.00$) between controls ($M = 123.4$, $SD = 5.21$) and HTD patients ($M = 121.32$, $SD = 11.24$).

6.3 | Heart rate, heart rate variability, and blood pressure results during HBD

Regarding HR and HRV, a one-way ANOVA for each measure showed no differences between samples during the IC (Table 1). Regarding blood pressure, one index was obtained with the format systolic/diastolic measure. A one-way ANOVA revealed no between-group differences (Table 1). Also, negative results were controlled by Bayes factor analyses, all of which yielded values under 1, supporting the null hypothesis. Bayes results are shown in Supporting Information, Table 6.

6.4 | ERP results

6.4.1 | Within-group comparisons

HEP modulations at the frontal ROI were significantly more negative for IC than EC in both groups, within the expected time-window (200–500 ms; Figure 3). Similar results were found in the right frontal, left frontal, and centro-frontal ROIs (Figure 2). All significant results had moderate effect sizes (d from 0.43 to 0.61; see Supporting Information, Table 7).

6.4.2 | Between-group comparisons

To assess whether HEP modulations differed between groups, we calculated the differences between the IC and the EC by subtracting each data point of each condition (thus, HEP modulations during EC were considered as a baseline condition) (García-Cordero et al., 2016; Leopold & Schandry, 2001; Yoris et al., 2017). Monte Carlo permutations showed that, relative to controls, HTD patients presented decreased HEP differences between IC and EC in the windows from 225 to 253 ms and from 425 to 499 ms (Figure 3). These results were mirrored in the other three frontal ROIs. For the right frontal ROI, differences in favor of controls were found in a window between 464 and 499 ms; for the left frontal ROI, differences emerged in from 229 to 241 ms and from 428 to 499 ms; finally, for the central frontal ROI, effects were found from 229 to 241 ms and from 248 and 499 ms. These results are detailed in Figure 2. Additionally, calculations of Cohen's d revealed moderate effect sizes (d from 0.24 to 0.39) for all the ROIs between the ~400 to ~500 ms. Results are shown in Supporting Information, Table 8.

6.5 | Association between interoceptive and neuroimaging measures

6.5.1 | VBM results

In the control group, we found a positive correlation between the gray matter volume of the bilateral insula and the subjects' IC performance (Figure 3 and Table 2). No such correlations were observed in HTD patients. We also calculated the effect size of the results of the correlation between VBM and IC performance. To this end, we extracted the grey matter volume for each subject per group based on a mask of the significant results of the analysis (bilateral insula) from controls. Then, we calculated a Spearman correlation between these values and the IC scores for each sample. In line with our voxel-wise analysis, the control

TABLE 3　Nonparametric Spearman correlations between functional connectivity measures and interoceptive accuracy

| | Correlation with interoceptive accuracy | | | |
| | Controls | | HTD patients | |
FC area	p value	Spearman R	p value	Spearman R
Right posterior insula	.03*	0.46	.87	−0.04
Left posterior insula	.41	0.19	.58	0.13
Right anterior insula	.21	0.29	.80	0.06
Left anterior insula	.88	0.03	.76	0.07
Right anterior cingular cortex	.1	−0.37	.88	0.03
Left anterior cingular cortex	.05*	−0.42	.64	0.11
Right somatosensorial cortex	.70	−0.09	.70	−0.09
Left somatosensorial cortex	.38	−0.20	.68	.1

The asterisk (*) indicates significant values.

group showed a correlation value of 0.79 (associated with a p value < .001), while the patient group exhibited a value of 0.10 (associated with a p = .67). Finally, to compare the correlation values between groups, we first multiplied, per subject, the IC score and grey-matter volume from the same mask used for the effect size analysis (significant results in the bilateral insula). Then, we conducted an ANOVA based on these values (one per subject), and found significant differences between groups ($F = 12.11$, $p < 0.01$, $\eta p^2 = 0.24$).

6.5.2 | Seed analysis results

In the control group, we found two ROIs whose connectivity with the seed (left insula) significantly correlated with the subjects' IC performance: (a) the right posterior insula ($R = 0.46$, $p = .03$), and (b) the left ACC ($R = −0.42$, $p = .05$). No significant associations with any ROI were observed in the HTD sample (Figure 3b,c and Table 3). To determine whether these relationships were statistically different between groups, we performed an ANOVA comparing the strength of association between IC scores and the ROIs' functional connectivity. To combine the association strength of both findings into a single score per subject, we first absolutized the functional connectivity values to ensure that these results were not biased by the cancellation of association strength given their opposite directions (positive for the right posterior insula, and negative for the left ACC). Then, we followed the same procedure used for VBM analysis to integrate functional connectivity and IC performance. This analysis showed significant differences between groups ($F = 6.85$. $p = .001$, $\eta p^2 = 0.08$).

7 | DISCUSSION

This is the first study assessing behavioral, electrophysiological, and neuroimaging correlates of interoception in neurocognitively normal HTD patients. Relative to controls, the patients showed selective behavioral difficulties in monitoring their own cardiac signals, alongside a partial reduction of task-related HEP modulations. Moreover, whereas interoceptive performance was associated with the volume and connectivity of the insula in healthy subjects, this association was

abolished in the patients. These results show that behavioral and neurophysiological disruptions of interoception may be present in patients with high blood pressure, beyond the possible role of other neurocognitive alterations. Our findings thus indicate that interoception could operate differently under normotensive versus hypertensive conditions, suggesting that extracerebral biodynamics could partially reflect the status of body–brain communication (Gallese & Sinigaglia, 2011; Goldman & de Vignemont, 2009).

7.1 | Interoceptive disruptions following autonomic alterations in HTD

Results from the HBD task revealed behavioral interoceptive deficits in HTD patients. While similar deficits have been reported in psychiatric (Dunn et al., 2007; Khalsa et al., 2015; Muller et al., 2015; Yoris et al., 2015, 2017) and neurological (García-Cordero et al., 2016; Khalsa et al., 2009a; Ricciardi et al., 2016a,b; Terhaar et al., 2012) disorders (for a review, see Yoris et al., in press), our finding stands out because these patients showed no brain atrophy (as measured through VBM), tract-level alterations (as assessed with DTI), or functional connectivity abnormalities. This algins with previous reports of interoceptive alterations in patients with peripheral and autonomic conditions, such as HTD (mixing non-treated/medicated patients) (Koroboki et al., 2010), diabetes (Leopold & Schandry, 2001), and high blood pressure (Fahrenberg et al., 1995). However, this is the first study to show that interoceptive impairments in HTD may not be epiphenomenal to general motor or attentional difficulties, given that their performance on the EC was spared. Neither can this deficit be attributed to executive dysfunction, as the patients showed normal scores in the neuropsychological assessment batteries. Taken together, these observations reveal a specific interoceptive deficit associated with peripheral disruptions in the cardiovascular system.

Moreover, although both groups showed the expected differences in HEP amplitude between conditions (García-Cordero et al., 2016; Leopold & Schandry, 2001), subtraction analysis revealed that such modulations were reduced in HTD patients (Figures 1 and 2). The HEP

is a robust cortical signature of interoception that accompanies behavioral deficits during the same HBD task in patients with neurological (García-Cordero et al., 2016; Leopold & Schandry, 2001; Yoris et al., 2017) and psychiatric (Muller et al., 2015; Schulz et al., 2015; Terhaar et al., 2012; Yoris et al., 2017) disorders. Thus, our results show that this cortical marker of interoception disrupted by brain damage may also be affected in patients with peripheral cardiac abnormalities. Conceivably, group differences in the HEP windows (around 200 and 500 ms) could be associated with cardiac systole/diastole contraction activity (Park et al., 2007). Given the patients' neurocognitive preservation, between-group differences could be linked to alterations in the patients' baroreceptors (Laurent et al., 2003; O'Rourke & Nichols, 2005). Although we lack data on the status of these vessels, previous research has consistently shown their involvement in HTD (Chapleau & Sabharwal, 2011). In addition, these mechanisms are linked to the functioning of interoceptive pathways (Critchley et al., 2004; Critchley & Harrison, 2013; Gray et al., 2007; Park et al., 2007), which reinforces our interpretation.

As observed earlier, HTD patients presented interoceptive deficits with no alterations in volumetric, tract-level, or functional connectivity measures. Once again, this suggests that alterations in the functional organization of the interoceptive network might be related to peripheral cardiac alterations. Yet, our evidence does not fully rule out a potential role of cerebral changes that might influence interoceptive performance. In fact, HTD may affect brain structure and function in early stages, and, in certain cases, vascular deregulation may actually originate in the brain (Jennings & Zanstra, 2009). Therefore, although our neuroimaging analysis showed no differences between patients and controls, the former may have presented subtle brain alterations not detected by our recording or analysis methods.

Still, the fact remains that patients performed normally in a series of general cognitive tasks tapping various domains (e.g., motor planning, working memory, and verbal memory), which weakens the likelihood of undetected neurological alterations. In sum, even though further research is needed, our findings highlight the relevance of peripheral mechanisms in the alteration of interoceptive signals. This conclusion aligns with evidence of HBD deficits and HEP alterations in patients with diabetes (Leopold & Schandry, 2001), a condition associated with the vagal denervation of the heart (Wheeler & Watkins, 1973). Compatibly, reduced HEP modulations were observed together with self-heart tracking deficits, despite preserved external-hearth tracking abilities, in a patient with an extracorporeal left-univentricular cardiac assist device (Couto et al., 2013). Of note, HEP alterations in our HTD sample emerged in different domain-relevant ROIs and during canonical time windows of the HEP (Canales-Johnson et al., 2015; Fukushima et al., 2011; Gray et al., 2007). These findings show that even the neurophysiological correlates of interoception may become dysfunctional in the presence of peripheral cardiac system abnormalities.

Furthermore, whereas controls showed an association between HBD performance and grey matter density in key interoceptive regions (in particular, the insula), no such correlations were found in HTD patients. A similar pattern emerged for connectivity analysis. Indeed,

interoceptive performance in controls was associated with functional connectivity between the left insula and both the right anterior insula and the left ACC, which aligns with previous results (Avery et al., 2014; García-Cordero et al., 2016; Simmons et al., 2013; Taylor, Seminowicz, & Davis, 2009). Instead, HTD patients presented no association between the functional connectivity of interoceptive regions and performance. Previous studies have shown that the anatomical and functional integrity of interoceptive regions is associated with interoceptive performance in neurodegenerative conditions (García-Cordero et al., 2016; Yoris et al., in press). However, as observed earlier, deficits in the present HTD sample are not due to overall volumetric or tract-level differences between groups. Once again, this suggests that alterations in the functional organization of the interoceptive network need not be associated with damage to relevant brain regions. Rather, they can also be associated with disruptions of cardiovascular mechanisms, reinforcing the view that interoceptive mechanisms may rely on a bidirectional brain–body interplay.

7.2 | Toward a body-based conception of embodied cognition

In the last decades, a wealth of evidence has accrued to show that cognitive functions are embodied, that is, grounded in experientially relevant biological mechanisms (Barsalou, 2008; Craig, 2009; Gallese & Lakoff, 2005; Mahon & Caramazza, 2008; Seth, 2013). However, this perspective has largely restricted such biological foundations to brain regions, especially within clinical research. Here we show that high-order domains, such as interoceptive processing, are not only rooted in functionally relevant neural systems, but also be in the very peripheral bodily systems supporting and informing such systems in the first place. Specifically, focusing on cardiac monitoring skills in HTD, we have shown that behavioral and neurocognitive markers of interoception can become distinctively altered if autonomic abnormalities are present, even in the absence of neuroanatomical or general cognitive impairment. These findings extend previous reports showing that different pharmacological (Khalsa et al., 2009a; Khalsa, Rudrauf, Sandesara, Olshansky, & Tranel, 2009b), physical (Williamson, Mccoll, Mathews, Ginsburg, & Mitchell, 1999; Williamson, Mccoll, & Mathews, 2003), and gut stimulation/deregulation (Aziz, 2012; Mayer & Tillisch, 2011) conditions are associated with the functioning of key interoceptive hubs (specially the insular cortex).

The peripheral model of interoception proposed here leads to specific hypotheses for a new research agenda. Critical evidence could be gained by comparing relevant behavioral and neurocognitive markers in patients before and after heart transplant, especially considering the disruption of vagal signaling during surgery and the potential for postoperative cardiac reinervation (Grupper, Gewirtz, & Kushwaha, 2017; Murphy et al., 2000), which could induce domain-relevant neuroplastic adaptations. In this sense, other peripheral procedures, like gastric distention insertion of gastric balloons, have been observed to trigger changes in interoceptive areas, such as the insula and the amygdala (Wang et al., 2008).

Furthermore, above and beyond this particular domain, our findings open exciting avenues to explore the role of extracerebral bodily systems as direct mediators of experientially relevant cognitive functions. Extant evidence shows that Botox-induced paralysis of relevant muscle groups can transiently impair recognition of verbal stimuli conveying negative emotions (Havas, Glenberg, Gutowski, Lucarelli, & Davidson, 2010). By the same token, building on evidence that words denoting bodily actions (Abrevaya et al., 2017; Bocanegra et al., 2015, 2017; García et al., 2017; García & Ibáñez, 2016; Melloni et al., 2015; Pulvermüller, 2005), smells (Gonzalez et al., 2006), and tastes (Barros-Loscertales et al., 2012) depend on brain regions subserving motor, olfactory, and gustatory functions, respectively, it could be hypothesized that such domains could be specifically affected in amputees (Flor, Elbert, Knecht, Wienbruch, & Pantev, 1995; Makin, Scholz, Henderson Slater, Johansen-Berg, & Tracey, 2015) and patients with hyposmia (Gaines, 2010; Guilemany et al., 2009; Henkin & Levy, 2002) or taste discrimination deficits (Eskine, Kacinik, & Prinz, 2011). These are just some of the several peripheral clinical models which could shed light on the apparently critical role of peripheral systems in grounding higher order cognitive skills. Such a conceptual recast could reveal the extent to which cognitive functions rely on relevant autonomic dynamics.

8 | LIMITATIONS AND AVENUES FOR FURTHER RESEARCH

The present work features some limitations and restrictions. First, it is based on a modest sample size. Note, however, that previous works on interoception have yielded replicable results with similar or smaller samples (Fahrenberg et al., 1995; Koroboki et al., 2010; Leopold & Schandry, 2001). Moreover, the consistency of our results across behavioral, electrophysiological, and anatomofunctional dimensions, with moderate to large effect sizes, further attests to their robustness. Still, future studies in this line should aim to recruit larger samples, ideally including subgroups with different forms of HTD.

Second, given our modest sample size, all neuroimaging results were reported with uncorrected statistical thresholds ($p < .001$ uncorrected with 50 voxels as extent threshold for the voxel-wise analysis, and $p \leq .05$ uncorrected for comparisons of average within ROIs). Despite the risk of false positive findings, there are several reasons that support the validity of this statistical approach. First, in assessing the patients' neurocognitive status, we intentionally used this permissive threshold for a whole-brain voxel-wise analysis –instead of an FWE or FDR corrections, which would restrict significant differences—to ensure that, despite the uncorrected approach, patients did not present any brain structural or functional alterations relative to controls—a similar strategy has been applied in a previous study (Sedeno et al., 2017). Then, for the regression results between morphometry and behavior, we kept the uncorrected threshold but restricted to the key interoceptive areas. This finding might not be considered as a potential false positive given that it is consistent with research showing the putative role of the insular cortex in interoception—also, we have employed a large voxel extent threshold (50 voxels) to prevent spurious findings, as

shown with 10 voxels (Poldrack et al., 2017). In addition, this uncorrected threshold has been used as a standard value in previous VBM and functional connectivity research (García-Cordero et al., 2016; Hassanpour et al., 2016; Irish et al., 2014; Kuehn, Mueller, Lohmann, & Schuetz-Bosbach, 2016; Markett et al., 2014; Melloni et al., 2016; Rabinovici et al., 2007; Sedeno et al., 2017; Simmons et al., 2013). Regarding the association between the seed-based analysis and behavior performance, we reduced the number of comparisons via averaging the correlation values within each interoceptive hub (comparisons went from a thousand to less than ten), and then applied a $p < .05$ uncorrected threshold, as in previous works (Abrevaya et al., 2017; Mayer et al., 2011; Wu et al., 2011a,b). Moreover, both regression analyses showed moderate to strong effect sizes only for the control group (controls, $R = 0.79$; HTD, $R = 0.1$), which supports the validity of our imaging results.

Another potential limitation is that fMRI data underlying our functional connectivity results come from a scanner with a low magnetic field (1.5 T). Though arguably suboptimal, our approach is certainly adequate, as shown by (a) multicenter studies combining equipment with different Teslas (Biswal et al., 2010; Dosenbach et al., 2010; Long et al., 2008; Power et al., 2011; Sedeno et al., 2017), and even showing the functional connectivity variability due to the magnetic field was relatively low (Biswal et al., 2010); (b) reports of consistent functional connectivity alterations in neuropsychiatric conditions obtained with 1.5 T scanners (Demirtas et al., 2016; García-Cordero et al., 2016; Hoekzema et al., 2014; Magioncalda et al., 2015; Melloni et al., 2016; Oldehinkel et al., 2016; Rolland et al., 2015; Sedeno et al., 2017; Wu et al., 2011a; Zalesky, Fornito, Egan, Pantelis, & Bullmore, 2012); and (c) several studies that reliably identified, characterized, and reproduced resting-state networks in healthy participants based on low-magnetic-field equipment (Biswal et al., 2010; Chou, Panych, Dickey, Petrella, & Chen, 2012; Power et al., 2011; Song, Panych, & Chen, 2016). Moreover, although the sensitivity and specificity of the BOLD signal is expected to improve as its strength increases (Duyn, 2012; Moseley, Liu, Rodriguez, & Brosnan, 2009; Triantafyllou, Hoge, & Wald, 2006), this enhancement is also associated with stronger physiological noise contribution in the signal (Kruger & Glover, 2001; Kruger, Kastrup, & Glover, 2001; Triantafyllou et al., 2005). Looking forward, even though our resting-state fMRI data prove adequate to perform our current analyses, future studies should assess the impact of different acquisition parameters on the assessment of functional networks in HTD patients.

Third, our findings may have been partially influenced by the patients' medication, whose effects on cognitive functions remain unclear (Tzourio et al., 1999). Yet, as we do not have clinical data from the patients prior to treatment, we cannot fully exclude physiological differences due to medication cessation. However, we were careful to suspend the medication intake 48hs before with the aim to reduce drug effects. In this sense, it would be interesting to extend the present research via direct comparisons of interoceptive mechanisms in treated and untreated HTD patients.

Finally, another limitation of our study is the difficulty to characterize a HTD sample avoiding cognitive and structural impairment. While

such deficits may emerge in older individuals, we strategically rejected all subjects with signs of neurocognitive abnormalities, resulting in a modest sample size. Yet, further research in this direction could assess a possible influence of such disruptions on the interoceptive profile of HTD patients, and compare relevant markers with those of other neurodegenerative diseases and/or cardiac syndromes.

9 | CONCLUSION

This study assessed interoception deficits in hypertensive patients with neurocognitive preservation. The deficits presented by the HTD sample indicate that neurocognitive markers of interoception could be disrupted in the presence of high blood pressure, despite antihypertensive treatment. This finding supports a broad vision of embodied cognition, suggesting that interoceptive signatures may partially depend on the integrity of the mind–body communication.

ORCID

Nicolás Lori http://orcid.org/0000-0002-5895-0880
Agustín Ibáñez http://orcid.org/0000-0001-6758-5101

REFERENCES

Abrevaya, S., Sedeno, L., Fitipaldi, S., Pineda, D., Lopera, F., Buritica, O., . . . Garcia, A. M. (2017). The road less traveled: Alternative pathways for action-verb processing in Parkinson's disease. *Journal of Alzheimer's Disease*, *55*, 1429–1435.

Adolfi, F., Couto, B., Richter, F., Decety, J., Lopez, J., Sigman, M., . . . Ibanez, A. (2016). Convergence of interoception, emotion, and social cognition: A twofold fMRI meta-analysis and lesion approach. *Cortex*, *88*, 124–142.

Amoruso, L., Sedeno, L., Huepe, D., Tomio, A., Kamienkowski, J., Hurtado, E., . . . Ibanez, A. (2014). Time to Tango: Expertise and contextual anticipation during action observation. *NeuroImage*, *98*, 366–385.

Anderson, J. L. R., Jenkinson, M., & Smith, S. (2007). Non-linear registration, aka Spatial normalisation FMRIB technical report TR07JA2. FMRIB Analysis Group of the University of Oxford, 2.

Andrillon, T., Kouider, S., Agus, T., & Pressnitzer, D. (2015). Perceptual learning of acoustic noise generates memory-evoked potentials. *Current Biology*, *25*, 2823–2829.

Ashburner, J. (2007). A fast diffeomorphic image registration algorithm. *NeuroImage*, *38*, 95–113.

Ashburner, J., & Friston, K. J. (1999). Nonlinear spatial normalization using basis functions. *Human Brain Mapping*, *7*, 254–266.

Ashburner, J., & Friston, K. J. (2000). Voxel-based morphometry–the methods. *NeuroImage*, *11*, 805–821.

Avery, J. A., Drevets, W. C., Moseman, S. E., Bodurka, J., Barcalow, J. C., & Simmons, W. K. (2014). Major depressive disorder is associated with abnormal interoceptive activity and functional connectivity in the insula. *Biological Psychiatry*, *76*, 258–266.

Aziz, Q. (2012). Brain–gut interactions in the regulation of satiety: New insights from functional brain imaging. *Gut*, gutjnl-2012–302368.

Barros-Loscertales, A., Gonzalez, J., Pulvermuller, F., Ventura-Campos, N., Bustamante, J. C., Costumero, V., . . . Avila, C. (2012). Reading salt activates gustatory brain regions: fMRI evidence for semantic grounding in a novel sensory modality. *Cerebral Cortex*, *22*, 2554–2563.

Barsalou, L. W. (2008). Grounded cognition. *Annual Review of Psychology*, *59*, 617–645.

Beck, A. T., Steer, R. A., Ball, R., & Ranieri, W. (1996). Comparison of Beck Depression Inventories -IA and -II in psychiatric outpatients. *Journal of Personality Assessment*, *67*, 588–597.

Behrens, T. E., Woolrich, M. W., Jenkinson, M., Johansen-Berg, H., Nunes, R. G., Clare, S., . . . Smith, S. M. (2003). Characterization and propagation of uncertainty in diffusion-weighted MR imaging. *Magnetic Resonance in Medicine*, *50*, 1077–1088.

Birba, A., Garcia-Cordero, I., Kozono, G., Legaz, A., Ibanez, A., Sedeno, L., & Garcia, A. M. (2017). Losing ground: Frontostriatal atrophy disrupts language embodiment in Parkinson's and Huntington's disease. *Neuroscience & Biobehavioral Reviews*, *80*, 673–687.

Biswal, B. B., Mennes, M., Zuo, X. N., Gohel, S., Kelly, C., Smith, S. M., . . . Milham, M. P. (2010). Toward discovery science of human brain function. *Proceedings of the National Academy of Sciences of the United States of America*, *107*, 4734–4739.

Bocanegra, Y., García, A. M., Lopera, F., Pineda, D., Baena, A., Ospina, P., . . . Ibáñez, A. (2017). Unspeakable motion: Selective action-verb impairments in Parkinson's disease patients without mild cognitive impairment. *Brain and Language*, *168*, 37–46.

Bocanegra, Y., García, A. M., Pineda, D., Buriticá, O., Villegas, A., Lopera, F., . . . Trujillo, N. (2015). Syntax, action verbs, action semantics, and object semantics in Parkinson's disease: Dissociability, progression, and executive influences. *Cortex*, *69*, 237–254.

Canales-Johnson, A., Silva, C., Huepe, D., Rivera-Rei, A., Noreika, V., Garcia, M. D., . . . Bekinschtein, T. A. (2015). Auditory feedback differentially modulates behavioral and neural markers of objective and subjective performance when tapping to your heartbeat. *Cerebral Cortex*, *25*, 4490–4503.

Chao-Gan, Y., & Yu-Feng, Z. (2010). DPARSF: A MATLAB toolbox for "Pipeline" data analysis of resting-state fMRI. *Frontiers in Systems Neuroscience*, *4*, 13.

Chapleau, M. W., & Sabharwal, R. (2011). Methods of assessing vagus nerve activity and reflexes. *Heart Failure Reviews*, *16*, 109–127.

Chou, Y. H., Panych, L. P., Dickey, C. C., Petrella, J. R., & Chen, N. K. (2012). Investigation of long-term reproducibility of intrinsic connectivity network mapping: A resting-state fMRI study. *AJNR American Journal of Neuroradiology*, *33*, 833–838.

Cohen, J. (1988). *Statistical power analysis for the behavioral sciences* (pp. 20–26). Hillsdale, NJ: Lawrence Earlbaum Associates.

Couto, B., Adolfi, F., Velasquez, M., Mesow, M., Feinstein, J., Canales-Johnson, A., . . . Ibanez, A. (2015). Heart evoked potential triggers brain responses to natural affective scenes: A preliminary study. *Autonomic Neuroscience*, *193*, 132–137.

Couto, B., Salles, A., Sedeno, L., Peradejordi, M., Barttfeld, P., Canales-Johnson, A., . . . Ibanez, A. (2013). The man who feels two hearts: The different pathways of interoception. *Social Cognitive and Affective Neuroscience*, *9.9*, 1253–1260.

Craig, A. D. (2002). How do you feel? Interoception: The sense of the physiological condition of the body. *Nature Reviews. Neuroscience, 3*, 655–666.

Craig, A. D. (2009). How do you feel–now? The anterior insula and human awareness. *Nature Reviews. Neuroscience, 10*, 59–70.

Critchley, H. D., & Harrison, N. A. (2013). Visceral influences on brain and behavior. *Neuron, 77*, 624–638.

Critchley, H. D., Wiens, S., Rotshtein, P., Ohman, A., & Dolan, R. J. (2004). Neural systems supporting interoceptive awareness. *Nature Neuroscience, 7*, 189–195.

DE Leeuw, F., DE Groot, J. C., Achten, E., Oudkerk, M., Ramos, L., Heijboer, R., ... Breteler, M. (2001). Prevalence of cerebral white matter lesions in elderly people: A population based magnetic resonance imaging study. The Rotterdam Scan Study. *Journal of Neurology, Neurosurgery & Psychiatry, 70*, 9–14.

DE Leeuw, F. E., DE Groot, J. C., Oudkerk, M., Witteman, J., Hofman, A., VAN Gijn, J., & Breteler, M. (2002). Hypertension and cerebral white matter lesions in a prospective cohort study. *Brain, 125*, 765–772.

Demirtas, M., Tornador, C., Falcon, C., Lopez-Sola, M., Hernandez-Ribas, R., Pujol, J., ... Deco, G. (2016). Dynamic functional connectivity reveals altered variability in functional connectivity among patients with major depressive disorder. *Human Brain Mapping, 37*, 2918–2930.

Dienes, Z. (2011). Bayesian versus orthodox statistics: Which side are you on? *Perspectives on Psychological Science, 6*, 274–290.

Dienes, Z. (2014). Using Bayes to get the most out of non-significant results. *Frontiers in Psychology, 5*.

Dienes, Z., Coulton, S., & Heather, N. (2017). Using Bayes factors to evaluate evidence for no effect: Examples from the SIPS project. *Addiction*.

Dienes, Z., & Mclatchie, N. (2017). Four reasons to prefer Bayesian analyses over significance testing. *Psychonomic Bulletin & Review*, 1–12.

Dosenbach, N. U., Nardos, B., Cohen, A. L., Fair, D. A., Power, J. D., Church, J. A., ... Schlaggar, B. L. (2010). Prediction of individual brain maturity using fMRI. *Science, 329*, 1358–1361.

Dunn, B. D., Dalgleish, T., Ogilvie, A. D., & Lawrence, A. D. (2007). Heartbeat perception in depression. *Behaviour Research and Therapy, 45*, 1921–1930.

Duyn, J. H. (2012). The future of ultra-high field MRI and fMRI for study of the human brain. *NeuroImage, 62*, 1241–1248.

Eckberg, D. L. (1997). Sympathovagal balance: A critical appraisal. *Circulation, 96*, 3224–3232.

Eskine, K. J., Kacinik, N. A., & Prinz, J. J. (2011). A bad taste in the mouth gustatory disgust influences moral judgment. *Psychological Science, 22*, 295–299.

Fahrenberg, J., Franck, M., Baas, U., & Jost, E. (1995). Awareness of blood pressure: Interoception or contextual judgement? *Journal of Psychosomatic Research, 39*, 11–18.

Fairclough, S. H., & Goodwin, L. (2007). The effect of psychological stress and relaxation on interoceptive accuracy: Implications for symptom perception. *Journal of Psychosomatic Research, 62*, 289–295.

Farmer, M. E., Kittner, S. J., Abbott, R. D., Wolz, M. M., Wolfs, P. A., & White, L. R. (1990). Longitudinally measured blood pressure, antihypertensive medication use, and cognitive performance: The Framingham Study. *Journal of Clinical Epidemiology, 43*, 475–480.

Flor, H., Elbert, T., Knecht, S., Wienbruch, C., & Pantev, C. (1995). Phantom-limb pain as a perceptual correlate of cortical reorganization following arm amputation. *Nature, 375*, 482.

Fox, M. D., Snyder, A. Z., Vincent, J. L., Corbetta, M., VAN Essen, D. C., & Raichle, M. E. (2005). The human brain is intrinsically organized into dynamic, anticorrelated functional networks. *Proceedings of the National Academy of Sciences of the United States of America, 102*, 9673–9678.

Fukushima, H., Terasawa, Y., & Umeda, S. (2011). Association between interoception and empathy: Evidence from heartbeat-evoked brain potential. *International Journal of Psychophysiology, 79*, 259–265.

Gaines, A. D. (2010). *Anosmia and hyposmia. Allergy and asthma proceedings* (pp. 185–189). OceanSide Publications, Inc..

Gallese, V., & Lakoff, G. (2005). The Brain's concepts: The role of the Sensory-motor system in conceptual knowledge. *Cognitive Neuropsychology, 22*, 455–479.

Gallese, V., & Sinigaglia, C. (2011). What is so special about embodied simulation? *Trends in Cognitive Sciences, 15*, 512–519.

Garcia, A. M., Abrevaya, S., Kozono, G., Cordero, I. G., Cordoba, M., Kauffman, M. A., ... Ibanez, A. (2017). The cerebellum and embodied semantics: Evidence from a case of genetic ataxia due to STUB1 mutations. *Journal of Medical Genetics, 54*, 114–124.

García, A. M., & Ibáñez, A. (2016). A touch with words: Dynamic synergies between manual actions and language. *Neuroscience & Biobehavioral Reviews, 68*, 59–95.

García, A. M., Sedeño, L., Trujillo, N., Bocanegra, Y., Gomez, D., Pineda, D., ... Ibáñez, A. (2017). Language deficits as a preclinical window into Parkinson's disease: Evidence from asymptomatic parkin and dardarin mutation carriers. *Journal of the International Neuropsychological Society, 23*, 150–158.

García-Cordero, I., Sedeño, L., DE LA Fuente, L., Slachevsky, A., Forno, G., Klein, F., ... Ibañez, A. (2016). Feeling, learning from and being aware of inner states: Interoceptive dimensions in neurodegeneration and stroke. *Philosophical Transactions of the Royal Society B: Biological Sciences, 371*, p. 20160006.

Garfinkel, S. N., Seth, A. K., Barrett, A. B., Suzuki, K., & Critchley, H. D. (2015). Knowing your own heart: Distinguishing interoceptive accuracy from interoceptive awareness. *Biological Psychology, 104*, 65–74.

Goldman, A., & DE Vignemont, F. (2009). Is social cognition embodied? *Trends in Cognitive Sciences, 13*, 154–159.

Gons, R. A., DE Laat, K. F., VAN Norden, A. G., VAN Oudheusden, L. J., VAN Uden, I. W., Norris, D. G., ... DE Leeuw, F.-E. (2010). Hypertension and cerebral diffusion tensor imaging in small vessel disease. *Stroke, 41*, 2801–2806.

Gonzalez, J., Barros-Loscertales, A., Pulvermuller, F., Meseguer, V., Sanjuan, A., Belloch, V., & Avila, C. (2006). Reading cinnamon activates olfactory brain regions. *NeuroImage, 32*, 906–912.

Good, C. D., Johnsrude, I. S., Ashburner, J., Henson, R. N., Friston, K. J., & Frackowiak, R. S. (2001). A voxel-based morphometric study of ageing in 465 normal adult human brains. *NeuroImage, 14*, 21–36.

Gray, M. A., Rylander, K., Harrison, N. A., Wallin, B. G., & Critchley, H. D. (2009). Following one's heart: Cardiac rhythms gate central initiation of sympathetic reflexes. *The Journal of Neuroscience, 29*, 1817–1825.

Gray, M. A., Taggart, P., Sutton, P. M., Groves, D., Holdright, D. R., Bradbury, D., ... Critchley, H. D. (2007). A cortical potential reflecting cardiac function. *Proceedings of the National Academy of Sciences of the United States of America, 104*, 6818–6823.

Grupper, A., Gewirtz, H., & Kushwaha, S. (2017). Reinnervation post-heart transplantation. *European Heart Journal*, e0hw604.

Guilemany, J. M., García, -Piñero, A., Alobid, I., Cardelús, S., Centellas, S., ... Mullol, J. (2009). Persistent allergic rhinitis has a moderate impact

on the sense of smell, depending on both nasal congestion and inflammation. *The Laryngoscope*, *119*, 233–238.

Hannesdottir, K., Nitkunan, A., Charlton, R. A., Barrick, T., Macgregor, G., & Markus, H. (2009). Cognitive impairment and white matter damage in hypertension: A pilot study. *Acta Neurologica Scandinavica*, *119*, 261–268.

Hassanpour, M. S., Yan, L., Wang, D. J., Lapidus, R. C., Arevian, A. C., Simmons, W. K., ... Khalsa, S. S. (2016). How the heart speaks to the brain: Neural activity during cardiorespiratory interoceptive stimulation. *Philosophical Transactions of the Royal Society B: Biological Sciences*, *371*, 20160017.

Havas, D. A., Glenberg, A. M., Gutowski, K. A., Lucarelli, M. J., & Davidson, R. J. (2010). Cosmetic use of botulinum toxin-A affects processing of emotional language. *Psychological Science*, *21*, 895–900.

Henkin, R. I., & Levy, L. M. (2002). Functional MRI of congenital hyposmia: Brain activation to odors and imagination of odors and tastes. *Journal of Computer Assisted Tomography*, *26*, 39–61.

Hoekzema, E., Carmona, S., Ramos-Quiroga, J. A., Richarte Fernandez, V., Bosch, R., Soliva, J. C., ... Vilarroya, O. (2014). An independent components and functional connectivity analysis of resting state fMRI data points to neural network dysregulation in adult ADHD. *Human Brain Mapping*, *35*, 1261–1272.

Mancia, G., De Backer, G., Dominiczak, A., Cifkova, R., Fagard, R., Germano, G., ... Management of Arterial Hypertension of the European Society of Hypertension; European Society of Cardiology. (2007). 2007 Guidelines for the management of arterial hypertension: The Task Force for the Management of Arterial Hypertension of the European Society of Hypertension (ESH) and of the European Society of Cardiology (ESC). *Journal of Hypertension*, *25*, 1105–1187.

Irish, M., Piguet, O., Hodges, J. R., & Hornberger, M. (2014). Common and unique gray matter correlates of episodic memory dysfunction in frontotemporal dementia and Alzheimer's disease. *Human Brain Mapping*, *35*, 1422–1435.

Jenkinson, M., & Smith, S. (2001). A global optimisation method for robust affine registration of brain images. *Medical Image Analysis*, *5*, 143–156.

Jennings, J. R., & Zanstra, Y. (2009). Is the brain the essential in hypertension? *NeuroImage*, *47*, 914–921.

Kern, M., Aertsen, A., Schulze-Bonhage, A., & Ball, T. (2013). Heart cycle-related effects on event-related potentials, spectral power changes, and connectivity patterns in the human ECoG. *NeuroImage*, *81*, 178–190.

Khalsa, S. S., Craske, M. G., Li, W., Vangala, S., Strober, M., & Feusner, J. D. (2015). Altered interoceptive awareness in anorexia nervosa: Effects of meal anticipation, consumption and bodily arousal. *International Journal of Eating Disorders*, *48*, 889–897.

Khalsa, S. S., Rudrauf, D., Feinstein, J. S., & Tranel, D. (2009a). The pathways of interoceptive awareness. *Nature Neuroscience*, *12*, 1494–1496.

Khalsa, S. S., Rudrauf, D., Sandesara, C., Olshansky, B., & Tranel, D. (2009b). Bolus isoproterenol infusions provide a reliable method for assessing interoceptive awareness. *International Journal of Psychophysiology*, *72*, 34–45.

Kilander, L., Nyman, H., Boberg, M., Hansson, L., & Lithell, H. (1998). Hypertension is related to cognitive impairment. *Hypertension*, *31*, 780–786.

Ko, D. T., Hebert, P. R., Coffey, C. S., Sedrakyan, A., Curtis, J. P., & Krumholz, H. M. (2002). βblocker therapy and symptoms of depression, fatigue, and sexual dysfunction. *JAMA*, *288*, 351–357.

Koroboki, E., Zakopoulos, N., Manios, E., Rotas, V., Papadimitriou, G., & Papageorgiou, C. (2010). Interoceptive awareness in essential hypertension. *International Journal of Psychophysiology*, *78*, 158–162.

Kruger, G., & Glover, G. H. (2001). Physiological noise in oxygenation-sensitive magnetic resonance imaging. *Magnetic Resonance in Medicine*, *46*, 631–637.

Kruger, G., Kastrup, A., & Glover, G. H. (2001). Neuroimaging at 1.5 T and 3.0 T: Comparison of oxygenation-sensitive magnetic resonance imaging. *Magnetic Resonance in Medicine*, *45*, 595–604.

Kuehn, E., Mueller, K., Lohmann, G., & Schuetz-Bosbach, S. (2016). Interoceptive awareness changes the posterior insula functional connectivity profile. *Brain Structure and Function*, *221*, 1555–1571.

Lakens, D. (2013). Calculating and reporting effect sizes to facilitate cumulative science: A practical primer for t-tests and ANOVAs. *Frontiers in Psychology*, *4*.

Launer, L. J., Masaki, K., Petrovitch, H., Foley, D., & Havlik, R. J. (1995). The association between midlife blood pressure levels and late-life cognitive function: The Honolulu-Asia Aging Study. *JAMA*, *274*, 1846–1851.

Laurent, S., Katsahian, S., Fassot, C., Tropeano, A.-I., Gautier, I., Laloux, B., & Boutouyrie, P. (2003). Aortic stiffness is an independent predictor of fatal stroke in essential hypertension. *Stroke*, *34*, 1203–1206.

Leopold, C., & Schandry, R. (2001). The heartbeat-evoked brain potential in patients suffering from diabetic neuropathy and in healthy control persons. *Clinical Neurophysiology*, *112*, 674–682.

Long, X. Y., Zuo, X. N., Kiviniemi, V., Yang, Y., Zou, Q. H., Zhu, C. Z., ... Zang, Y. F. (2008). Default mode network as revealed with multiple methods for resting-state functional MRI analysis. *Journal of Neuroscience Methods*, *171*, 349–355.

Magioncalda, P., Martino, M., Conio, B., Escelsior, A., Piaggio, N., Presta, A., ... Amore, M. (2015). Functional connectivity and neuronal variability of resting state activity in bipolar disorder–reduction and decoupling in anterior cortical midline structures. *Human Brain Mapping*, *36*, 666–682.

Mahon, B. Z., & Caramazza, A. (2008). A critical look at the embodied cognition hypothesis and a new proposal for grounding conceptual content. *Journal of Physiology - Paris*, *102*, 59–70.

Makin, T. R., Scholz, J., Henderson Slater, D., Johansen-Berg, H., & Tracey, I. (2015). Reassessing cortical reorganization in the primary sensorimotor cortex following arm amputation. *Brain*, *138*, 2140–2146.

Manly, B. F. J. (2007). *Randomization, bootstrap, and Monte Carlo methods in biology*. Boca Raton, FL: Chapman & Hall/CRC.

Markett, S., Reuter, M., Montag, C., Voigt, G., Lachmann, B., Rudorf, S., ... Weber, B. (2014). Assessing the function of the fronto-parietal attention network: Insights from resting-state fMRI and the attentional network test. *Human Brain Mapping*, *35*, 1700–1709.

Mayer, A. R., Mannell, M. V., Ling, J., Gasparovic, C., & Yeo, R. A. (2011). Functional connectivity in mild traumatic brain injury. *Human Brain Mapping*, *32*, 1825–1835.

Mayer, E. A., & Tillisch, K. (2011). The brain-gut axis in abdominal pain syndromes. *Annual Review of Medicine*, *62*, 381–396.

Melloni, M., Billeke, P., Baez, S., Hesse, E., DE LA Fuente, L., Forno, G., ... Ibanez, A. (2016). Your perspective and my benefit: Multiple lesion models of self-other integration strategies during social bargaining. *Brain*, p.aww231.

Melloni, M., Sedeno, L., Couto, B., Reynoso, M., Gelormini, C., Favaloro, R., ... Ibanez, A. (2013). Preliminary evidence about the effects of meditation on interoceptive sensitivity and social cognition. *Behavioral and Brain Functions*, *9*, 47.

Melloni, M., Sedeño, L., Hesse, E., García-Cordero, I., Mikulan, E., Plastino, A., … Lopera, F. (2015). Cortical dynamics and subcortical signatures of motor-language coupling in Parkinson's disease. *Scientific Reports*, 5.

Montoya, P., Schandry, R., & Muller, A. (1993). Heartbeat evoked potentials (HEP): Topography and influence of cardiac awareness and focus of attention. *Electroencephalography and Clinical Neurophysiology*, 88, 163–172.

Moseley, M. E., Liu, C., Rodriguez, S., & Brosnan, T. (2009). Advances in magnetic resonance neuroimaging. *Neurologic Clinics*, 27, 1–19, xiii.

Muller, L. E., Schulz, A., Andermann, M., Gabel, A., Gescher, D. M., Spohn, A., … Bertsch, K. (2015). Cortical representation of afferent bodily signals in Borderline Personality disorder: Neural correlates and relationship to emotional dysregulation. *JAMA Psychiatry*, 72, 1077–1086.

Murphy, D. A., Thompson, G. W., Ardell, J. L., Mccraty, R., Stevenson, R. S., Sangalang, V. E., … Smith, F. M. (2000). The heart reinnervates after transplantation. *Annals of Thoracic Surgery*, 69, 1769–1781.

Naccache, L., Gaillard, R., Adam, C., Hasboun, D., Clemenceau, S., Baulac, M., … Cohen, L. (2005). A direct intracranial record of emotions evoked by subliminal words. *Proceedings of the National Academy of Sciences of the United States of America*, 102, 7713–7717.

Nichols, T. E., DAS, S., Eickhoff, S. B., Evans, A. C., Glatard, T., Hanke, M., … Yeo, B. T. (2017). Best practices in data analysis and sharing in neuroimaging using MRI. *Nature Neuroscience*, 20, 299–303.

Nichols, T. E., & Holmes, A. P. (2002). Nonparametric permutation tests for functional neuroimaging: A primer with examples. *Human Brain Mapping*, 15, 1–25.

Nitkunan, A., Charlton, R. A., Mcintyre, D. J., Barrick, T. R., Howe, F. A., & Markus, H. S. (2008). Diffusion tensor imaging and MR spectroscopy in hypertension and presumed cerebral small vessel disease. *Magnetic Resonance in Medicine*, 59, 528–534.

O'rourke, M. F., & Nichols, W. W. (2005). Aortic diameter, aortic stiffness, and wave reflection increase with age and isolated systolic hypertension. *Hypertension*, 45, 652–658.

Oldehinkel, M., Beckmann, C. F., Franke, B., Hartman, C. A., Hoekstra, P. J., Oosterlaan, J., … Mennes, M. (2016). Functional connectivity in cortico-subcortical brain networks underlying reward processing in attention-deficit/hyperactivity disorder. *NeuroImage. Clinical*, 12, 796–805.

Oppenheimer, S., & Cechetto, D. (2016). The insular cortex and the regulation of cardiac function. *Comprehensive Physiology*, 15, 1081–1133.

Park, H.-D., Bernasconi, F., Salomon, R., Tallon-Baudry, C., Spinelli, L., Seeck, M., … Blanke, O. (2007). Neural sources and underlying mechanisms of neural responses to heartbeats, and their role in bodily self-consciousness: An intracranial EEG study. *Cerebral Cortex*, 1–14.

Park, H. D., Correia, S., Ducorps, A., & Tallon-Baudry, C. (2014). Spontaneous fluctuations in neural responses to heartbeats predict visual detection. *Nature Neuroscience*, 17, 612–618.

Poldrack, R. A., Baker, C. I., Durnez, J., Gorgolewski, K. J., Matthews, P. M., Munafo, M. R., … Yarkoni, T. (2017). Scanning the horizon: Towards transparent and reproducible neuroimaging research. *Nature Reviews. Neuroscience*, 18, 115–126.

Pollatos, O., Gramann, K., & Schandry, R. (2007a). Neural systems connecting interoceptive awareness and feelings. *Human Brain Mapping*, 28, 9–18.

Pollatos, O., Herbert, B. M., Kaufmann, C., Auer, D. P., & Schandry, R. (2007b). Interoceptive awareness, anxiety and cardiovascular reactivity to isometric exercise. *International Journal of Psychophysiology*, 65, 167–173.

Pollatos, O., Kirsch, W., & Schandry, R. (2005a). Brain structures involved in interoceptive awareness and cardioafferent signal processing: A dipole source localization study. *Human Brain Mapping*, 26, 54–64.

Pollatos, O., Kirsch, W., & Schandry, R. (2005b). On the relationship between interoceptive awareness, emotional experience, and brain processes. *Brain Research. Cognitive Brain Research*, 25, 948–962.

Pollatos, O., & Schandry, R. (2004). Accuracy of heartbeat perception is reflected in the amplitude of the heartbeat-evoked brain potential. *Psychophysiology*, 41, 476–482.

Power, J. D., Cohen, A. L., Nelson, S. M., Wig, G. S., Barnes, K. A., Church, J. A., … Petersen, S. E. (2011). Functional network organization of the human brain. *Neuron*, 72, 665–678.

Pulvermüller, F. (2005). Brain mechanisms linking language and action. *Nature Reviews. Neuroscience*, 6, 576–582.

Rabinovici, G. D., Seeley, W. W., Kim, E. J., Gorno-Tempini, M. L., Rascovsky, K., Pagliaro, T. A., … Rosen, H. J. (2007). Distinct MRI atrophy patterns in autopsy-proven Alzheimer's disease and frontotemporal lobar degeneration. *American Journal of Alzheimer's Disease & Other Dementias*, 22, 474–488.

Raglin, J. S., & Morgan, W. P. (1987). Influence of exercise and quiet rest on state anxiety and blood pressure. *Medicine & Science in Sports & Exercise*,

Raichle, M. E. (2009). A paradigm shift in functional brain imaging. *The Journal of Neuroscience*, 29, 12729–12734.

Räikkönen, K., Matthews, K. A., Flory, J. D., Owens, J. F., & Gump, B. B. (1999). Effects of optimism, pessimism, and trait anxiety on ambulatory blood pressure and mood during everyday life. *Journal of Personality and Social Psychology*, 76, 104.

Ricciardi, L., Demartini, B., Crucianelli, L., Krahé, C., Edwards, M. J., & Fotopoulou, A. (2016a). Interoceptive awareness in patients with functional neurological symptoms. *Biological Psychology*, 113, 68–74.

Ricciardi, L., Ferrazzano, G., Demartini, B., Morgante, F., Erro, R., Ganos, C., … Edwards, M. (2016b). Know thyself: Exploring interoceptive sensitivity in Parkinson's disease. *Journal of Neurological Sciences*, 364, 110–115.

Rolland, B., Amad, A., Poulet, E., Bordet, R., Vignaud, A., Bation, R., … Jardri, R. (2015). Resting-state functional connectivity of the nucleus accumbens in auditory and visual hallucinations in schizophrenia. *Schizophrenia Bulletin*, 41, 291–299.

Rouder, J. N., Speckman, P. L., Sun, D., Morey, R. D., & Iverson, G. (2009). Bayesian t tests for accepting and rejecting the null hypothesis. *Psychonomic Bulletin &Amp; Review*, 16, 225–237.

Sanchez, R. A., Ramos, F., Giannone, C., Fischer, P., Masnatta, L., Baglivo, H. P., … Hollenberg, N. K. (2003). Parallel renal and extremity blood supply abnormalities in nonmodulation: Responses to ACE inhibition. *Hypertension*, 41, 919–924.

Santamaria-Garcia, H., Baez, S., Reyes, P., Santamaria-Garcia, J. A., Santacruz-Escudero, J. M., Matallana, D., … Ibanez, A. (2017). A lesion model of envy and Schadenfreude: Legal, deservingness and moral dimensions as revealed by neurodegeneration. *Brain*, 140, 3357–3377.

Schandry, R. (1981). Heart beat perception and emotional experience. *Psychophysiology*, 18, 483–488.

Schandry, R., & Montoya, P. (1996). Event-related brain potentials and the processing of cardiac activity. *Biological Psychology*, 42, 75–85.

Scherr, P. A., Hebert, L. E., Smith, L. A., & Evans, D. A. (1991). Relation of blood pressure to cognitive function in the elderly. *American Journal of Epidemiology*, *134*, 1303–1315.

Schmidt, M. (1996). *Rey auditory verbal learning test: RAVLT: A handbook*. Western Psychological Services.

Schulz, A., Koster, S., Beutel, M. E., Schachinger, H., Vogele, C., Rost, S., ... Michal, M. (2015). Altered patterns of heartbeat-evoked potentials in depersonalization/derealization disorder: Neurophysiological evidence for impaired cortical representation of bodily signals. *Psychosomatic Medicine*, *77*, 506–516.

Schulz, S. M. (2016). Neural correlates of heart-focused interoception: A functional magnetic resonance imaging meta-analysis. *Philosophical Transactions of the Royal Society B: Biological Sciences*, *371*, 20160018.

Sedeno, L., Couto, B., Garcia-Cordero, I., Melloni, M., Baez, S., Morales Sepulveda, J. P., ... Ibanez, A. (2016). Brain network organization and social executive performance in frontotemporal dementia. *Journal of the International Neuropsychological Society*, *22*, 250–262.

Sedeno, L., Couto, B., Melloni, M., Canales-Johnson, A., Yoris, A., Baez, S., ... Ibanez, A. (2014). How do you feel when you can't feel your body? Interoception, functional connectivity and emotional processing in depersonalization-derealization disorder. *PLoS One*, *9*, e98769.

Sedeno, L., Piguet, O., Abrevaya, S., Desmaras, H., Garcia-Cordero, I., Baez, S., ... Ibanez, A. (2017). Tackling variability: A multicenter study to provide a gold-standard network approach for frontotemporal dementia. *Human Brain Mapping*, *38*, 3804–3822.

Seth, A. K. (2013). Interoceptive inference, emotion, and the embodied self. *Trends in Cognitive Sciences*, *17*, 565–573.

Shivkumar, K., Ajijola, O. A., Anand, I., Armour, J. A., Chen, P. S., Esler, M., ... Harper, R. M. (2016). Clinical neurocardiology defining the value of neuroscience-based cardiovascular therapeutics. *The Journal of Physiology*, *594*, 3911–3954.

Simmons, W. K., Avery, J. A., Barcalow, J. C., Bodurka, J., Drevets, W. C., & Bellgowan, P. (2013). Keeping the body in mind: Insula functional organization and functional connectivity integrate interoceptive, exteroceptive, and emotional awareness. *Human Brain Mapping*, *34*, 2944–2958.

Smith, R., Thayer, J. F., Khalsa, S. S., & Lane, R. D. (2017). The hierarchical basis of neurovisceral integration. *Neuroscience & Biobehavioral Reviews*.

Smith, S. M. (2002). Fast robust automated brain extraction. *Human Brain Mapping*, *17*, 143–155.

Smith, S. M., Jenkinson, M., Johansen-Berg, H., Rueckert, D., Nichols, T. E., Mackay, C. E., ... Behrens, T. E. (2006). Tract-based spatial statistics: Voxelwise analysis of multi-subject diffusion data. *NeuroImage*, *31*, 1487–1505.

Smith, S. M., Jenkinson, M., Woolrich, M. W., Beckmann, C. F., Behrens, T. E., Johansen-Berg, H., ... Matthews, P. M. (2004). Advances in functional and structural MR image analysis and implementation as FSL. *NeuroImage*, *23 Suppl 1*, S208–S219.

Song, X., Panych, L. P., & Chen, N. K. (2016). Data-driven and predefined ROI-based quantification of long-term resting-state fMRI reproducibility. *Brain Connect*, *6*, 136–151.

Spielberger, C. D., & Vagg, P. R. (1984). Psychometric properties of the STAI: A reply to Ramanaiah, Franzen, and Schill. *Journal of Personality Assessment*, *48*, 95–97.

Starr, J. M., Whalley, L. J., Inch, S., & Shering, P. (1993). Blood pressure and cognitive function in healthy old people. *Journal of the American Geriatrics Society*, *41*, 753–756.

Sullivan, P., Schoentgen, S., Dequattro, V., Procci, W., Levine, D., VAN DER Meulen, J., & Bornheimer, J. (1981). Anxiety, anger, and neurogenic tone at rest and in stress in patients with primary hypertension. *Hypertension*, *3*, II-119.

Szczepanski, S. M., Crone, N. E., Kuperman, R. A., Auguste, K. I., Parvizi, J., & Knight, R. T. (2014). Dynamic changes in phase-amplitude coupling facilitate spatial attention control in fronto-parietal cortex. *PLoS Biology*, *12*, e1001936.

Tarvainen, M. P., Niskanen, J. P., Lipponen, J. A., Ranta-Aho, P. O., & Karjalainen, P. A. (2013). Kubios HRV - Heart rate variability analysis software. *Computer methods and programs in biomedicine*, *113*, 210–220.

Taylor, K. S., Seminowicz, D. A., & Davis, K. D. (2009). Two systems of resting state connectivity between the insula and cingulate cortex. *Human Brain Mapping*, *30*, 2731–2745.

Terhaar, J., Viola, F. C., Bär, K.-J., & Debener, S. (2012). Heartbeat evoked potentials mirror altered body perception in depressed patients. *Clinical Neurophysiology*, *123*, 1950–1957.

Torralva, T., Roca, M., Gleichgerrcht, E., Lopez, P., & Manes, F. (2009). INECO Frontal Screening (IFS): A brief, sensitive, and specific tool to assess executive functions in dementia. *Journal of the International Neuropsychological Society*, *15*, 777–786.

Triantafyllou, C., Hoge, R. D., Krueger, G., Wiggins, C. J., Potthast, A., Wiggins, G. C., & Wald, L. L. (2005). Comparison of physiological noise at 1.5 T, 3 T and 7 T and optimization of fMRI acquisition parameters. *NeuroImage*, *26*, 243–250.

Triantafyllou, C., Hoge, R. D., & Wald, L. L. (2006). Effect of spatial smoothing on physiological noise in high-resolution fMRI. *NeuroImage*, *32*, 551–557.

Tzourio, C., Dufouil, C., Ducimetiere, P., & Alperovitch, A. (1999). Cognitive decline in individuals with high blood pressure: A longitudinal study in the elderly. EVA Study Group. *Epidemiology of Vascular Aging. Neurology*, *53*, 1948–1952.

Tzourio-Mazoyer, N., Landeau, B., Papathanassiou, D., Crivello, F., Etard, O., Delcroix, N., ... Joliot, M. (2002). Automated anatomical labeling of activations in SPM using a macroscopic anatomical parcellation of the MNI MRI single-subject brain. *NeuroImage*, *15*, 273–289.

VAN Boxtel, M. P., Gaillard, C., Houx, P. J., Buntinx, F., DE Leeuw, P. W., & Jolles, J. (1997). Can the blood pressure predict cognitive task performance in a healthy population sample? *Journal of Hypertension*, *15*, 1069–1076.

Wang, G. J., Tomasi, D., Backus, W., Wang, R., Telang, F., Geliebter, A., ... Volkow, N. D. (2008). Gastric distention activates satiety circuitry in the human brain. *NeuroImage*, *39*, 1824–1831.

Wang, X. H., Li, L., Xu, T., & Ding, Z. (2015). Investigating the temporal patterns within and between intrinsic connectivity networks under eyes-open and eyes-closed resting states: A dynamical functional connectivity study based on phase synchronization. *PLoS One*, *10*, e0140300.

Wheeler, T., & Watkins, P. (1973). Cardiac denervation in diabetes. *British Medical Journal*, *4*, 584–586.

WHO (1992). *The ICD-10 classification of mental and behavioural disorders: Clinical descriptions and diagnostic guidelines*. World Health Organization.

Williamson, J., Mccoll, R., Mathews, D., Ginsburg, M., & Mitchell, J. (1999). Activation of the insular cortex is affected by the intensity of exercise. *Journal of Applied Physiology (Bethesda, MD: 1985)*, *87*, 1213–1219.

Williamson, J. W., Mccoll, R., & Mathews, D. (2003). Evidence for central command activation of the human insular cortex during exercise. *Journal of Applied Physiology*, *94*, 1726–1734.

Winkler, A. M., Ridgway, G. R., Webster, M. A., Smith, S. M., & Nichols, T. E. (2014). Permutation inference for the general linear model. *NeuroImage*, *92*, 381–397.

Wu, T., Long, X., Wang, L., Hallett, M., Zang, Y., Li, K., & Chan, P. (2011a). Functional connectivity of cortical motor areas in the resting state in Parkinson's disease. *Human Brain Mapping*, *32*, 1443–1457.

Wu, X., Li, R., Fleisher, A. S., Reiman, E. M., Guan, X., Zhang, Y., . . . Yao, L. (2011b). Altered default mode network connectivity in Alzheimer's disease—a resting functional MRI and Bayesian network study. *Human Brain Mapping*, *32*, 1868–1881.

Xu, P., Huang, R., Wang, J., VAN Dam, N. T., Xie, T., Dong, Z., . . . Luo, Y. J. (2014). Different topological organization of human brain functional networks with eyes open versus eyes closed. *NeuroImage*, *90*, 246–255.

Yoris, A., Esteves, S., Couto, B., Melloni, M., Kichic, R., Cetkovich, M., . . . Sedeno, L. (2015). The roles of interoceptive sensitivity and metacognitive interoception in panic. *Behavioral and Brain Functions*, *11*, 14.

Yoris, A., García, A., Traiber, L., Santamaría-García, H., Martorell, M., Alifano, F., . . . Manes, F. (2017). The inner world of overactive monitoring: Neural markers of interoception in obsessive–compulsive disorder. *Psychological Medicine*, 1–14.

Yoris, A., García, A. M., Salamone, P., Sedeño, L., García-Cordero, I., & Ibáñez, A. (in press). Cardiac interoception in neurological conditions and its relevance for dimensional approaches. *In*: TSAKIRIS, M. & DE PREESTER, H. E. (eds.) *The Interoceptive Basis of the Mind*. Oxford, UK: Oxford University Press.

Zalesky, A., Fornito, A., Egan, G. F., Pantelis, C., & Bullmore, E. T. (2012). The relationship between regional and inter-regional functional connectivity deficits in schizophrenia. *Human Brain Mapping*, *33*, 2535–2549.

Zou, Q., Miao, X., Liu, D., Wang, D. J., Zhuo, Y., & Gao, J. H. (2015). Reliability comparison of spontaneous brain activities between BOLD and CBF contrasts in eyes-open and eyes-closed resting states. *NeuroImage*, *121*, 91–105.

SUPPORTING INFORMATION

Additional Supporting Information may be found online in the supporting information tab for this article.